

ECG SIGNAL PROCESSING AND ARRHYTHMIA DETECTION

Abstract

Automatic recognition of cardiac arrhythmias is important for diagnosis of cardiac abnormalities. Several algorithms have been proposed to classify ECG arrhythmias; however, they cannot perform very well. Therefore, in this presentation an expert system for ElectroCardioGram (ECG) arrhythmia classification is proposed. Discrete wavelet transform is used for processing ECG recordings, and extracting some features, and the Support Vector Machine (SVM) machine learning classifier performs the classification task. Two types of arrhythmias can be detected by the proposed system. Some recordings of the MIT-BIH arrhythmia database and real time patient heart beats (ECG Signals) have been used for filtering and analyzing.

Chapter 1

Introduction

1.1 ECG (Electrocardiography)

Electrocardiography is the process of producing an electrocardiogram (ECG or EKG), a recording - a graph of voltage versus time - of the electrical activity of the heart using electrodes placed on the skin. These electrodes detect the small electrical changes that are a consequence of cardiac muscle depolarization followed by repolarization during each cardiac cycle (heartbeat). Changes in the normal ECG pattern occur in numerous cardiac abnormalities, including cardiac rhythm disturbances (such as atrial fibrillation and ventricular tachycardia), inadequate coronary artery blood flow (such as myocardial ischemia and myocardial infarction), and electrolyte disturbances (such as hypokalemia and hyperkalemia).

In a conventional 12-lead ECG, ten electrodes are placed on the patient's limbs and on the surface of the chest. The overall magnitude of the heart's electrical potential is then measured from twelve different angles ("leads") and is recorded over a period of time (usually ten seconds). In this way, the overall magnitude and direction of the heart's electrical depolarization is captured at each moment throughout the cardiac cycle.

There are three main components to an ECG: the P wave, which represents the depolarization of the atria; the QRS complex, which represents the depolarization of the ventricles; and the T wave, which represents the repolarization of the ventricles.

During each heartbeat, a healthy heart has an orderly progression of depolarization that starts with pacemaker cells in the sinoatrial node, spreads throughout the atrium, passes through the atrioventricular node down into the bundle of His and into the Purkinje fibers, spreading down and to the left throughout the ventricles. This orderly pattern of depolarization gives rise to the

characteristic ECG tracing. To the trained clinician, an ECG conveys a large amount of information about the structure of the heart and the function of its electrical conduction system. Among other things, an ECG can be used to measure the rate and rhythm of heartbeats, the size and position of the heart chambers, the presence of any damage to the heart's muscle cells or conduction system, the effects of heart drugs, and the function of implanted pacemakers.

The ECG device detects and amplifies the tiny electrical changes on the skin that are caused when the heart muscle depolarizes during each heartbeat. At rest, each heart muscle cell has a negative charge, called the membrane potential, across its cell membrane. Decreasing this negative charge toward zero, via the influx of the positive cations, Na^+ and Ca^{++} , is called depolarization, which activates the mechanisms in the cell that cause it to contract. During each heartbeat, a healthy heart will have an orderly progression of a wave of depolarization that is triggered by the cells in the sinoatrial node, spreads out through the atrium, passes through the atrioventricular node and then spreads all over the ventricles. This is detected as tiny rises and falls in the voltage between two electrodes placed either side of the heart, which is displayed as a wavy line either on a screen or on paper. This display indicates the overall rhythm of the heart and weaknesses in different parts of the heart muscle.

1.2 QRS Complex in ECG Waveform

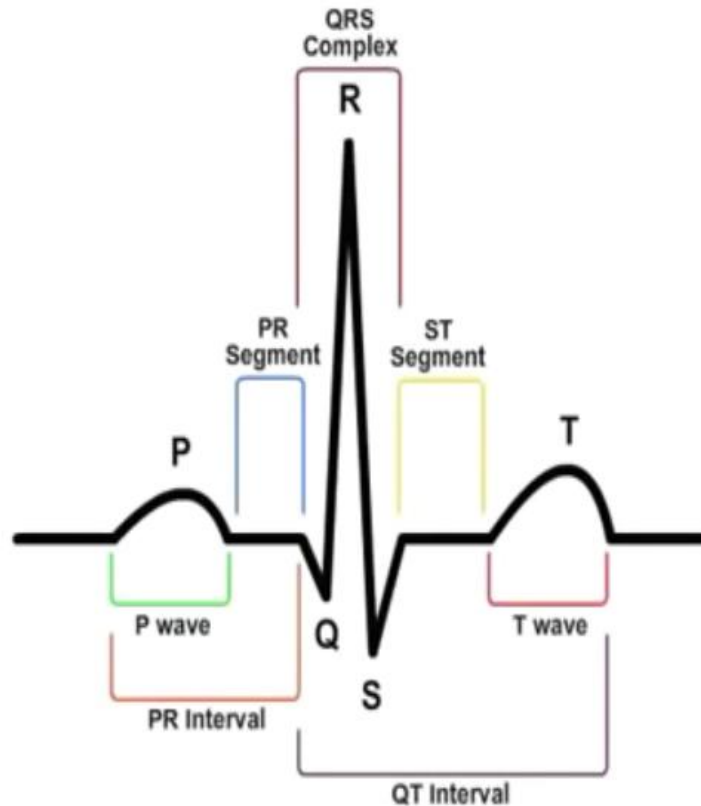


Fig 1.1 One Cycle of Heart Beat

A typical ECG consists of P-Q, Q-R-S and S-T segments whose duration and amplitude determine a lot of heart conditions and comprehensive and deep study is possible. The “**QRS Complex**” is a name for the combination of three of the graphical deflections seen on typical ECG. It corresponds to the depolarization of the right and left ventricles of the heart. In adults, it normally lasts 0.06 - 0.10 s. QRS duration of more than 120 ms represents a risk of heart attack and wide QRS is common in Heart Patients. ECG waveform can be used to determine the health of patient's heart. ECG can easily detect heart failure or heart attacks. For example ST segment above and below base-line shows possibility of heart failure or heart attack. Similarly we can

determine a healthy heart condition from ECG. The below figure shows ECG of patient with normal heart condition as well as with possibilities of heart failure.

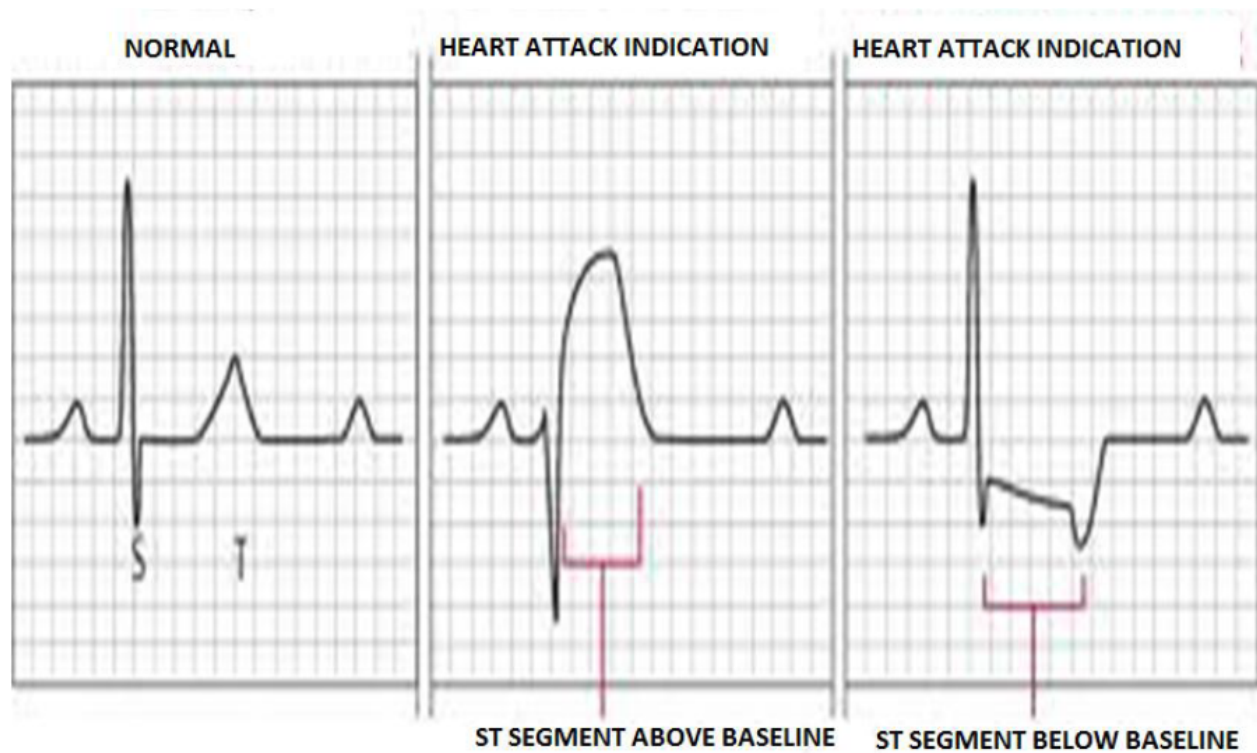


Fig 1.2 ECG Waveform during Heart Attack.

Feature	Description	Duration
RR interval	The interval between an R wave and the next R wave is the inverse of the heart rate. Normal resting heart rate is between 50 and 100 bpm	0.6 to 1.2s
P wave	During normal atrial depolarization, the main electrical vector is directed from the SA node towards the AV node, and spreads from the right atrium to the left atrium. This turns into the P wave on the ECG.	80ms
PR interval	The PR interval is measured from the beginning of the P wave to the beginning of the QRS complex. The PR interval reflects the time the electrical impulse takes to travel from the sinus node through the AV node and entering the ventricles. The PR interval is therefore a good estimate of AV node function.	120 to 200ms
PR segment	The PR segment connects the P wave and the QRS complex. This coincides with the electrical conduction from the AV node to the bundle of His to the bundle branches and then to the Purkinje Fibers. This electrical activity does not produce a contraction directly and is merely traveling down towards the ventricles and this shows up flat on the ECG. The PR interval is more clinically relevant.	50 to 120ms
QRS complex	The QRS complex reflects the rapid depolarization of the right and left ventricles. They have a large muscle mass compared to the atria and so the QRS complex usually has a much larger amplitude than the P-wave.	80 to 120ms
J-point	The point at which the QRS complex finishes and the ST segment begins. Used to measure the degree of ST elevation or depression present.	N/A

Table 1.1 Characteristics of QRS Complex

Feature	Description	Duration
ST segment	The ST segment connects the QRS complex and the T wave. The ST segment represents the period when the ventricles are depolarized. It is isoelectric.	80 to 120ms
T wave	The T wave represents the repolarization (or recovery) of the ventricles. The interval from the beginning of the QRS complex to the apex of the T wave is referred to as the <i>absolute refractory period</i> . The last half of the T wave is referred to as the <i>relative refractory period</i> (or vulnerable period).	160ms
ST interval	The ST interval is measured from the J point to the end of the T wave.	320ms
QT interval	The QT interval is measured from the beginning of the QRS complex to the end of the T wave. A prolonged QT interval is a risk factor for ventricular tachyarrhythmia and sudden death. It varies with heart rate and for clinical relevance requires a correction for this, giving the QTc.	300 to 430ms
U wave	The U wave is not always seen. It is typically low amplitude, and, by definition, follows the T wave.	

Table 1.2 Various Conditions for Different Ranges of Heartbeat.

Chapter 2

Noise Analysis in ECG Signals

2.1 ECG Denoising

The noise reduction in electrocardiography signals is one of the important problems, which appear during the analysis of ECG data. ECG signal is non-stationary biological signal in nature and plays a big role in diagnostics of human diseases. Therefore the electrocardiography signals need an effective denoising.

2.2 Various Noises present in ECG Signal

There are various types of noises present in ECG signals. The most commonly encountered noises are as follows:

2.2.1 Power line interference

Power line interference includes 50 Hz frequency components and harmonics which can be modeled as sinusoids and combination of sinusoids that interface with the ECG signal as noise. Since Signal to Noise Ratio (SNR) of electrocardiogram signal is very low due to the effect of noise, the interfering frequency at 50 Hz may overwhelm the source signal.

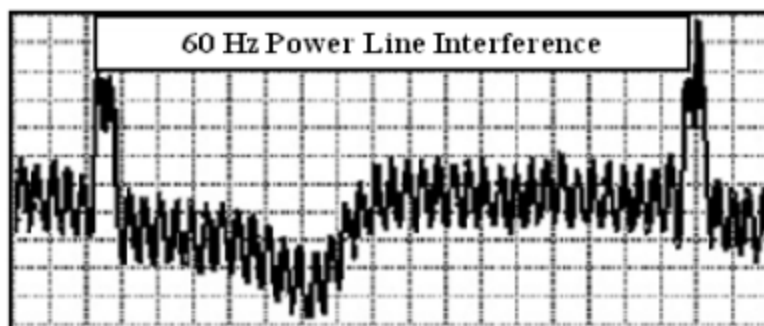


Fig 2.1 Power Line Interface Noise

2.2.2 Electrode contact noise

Electrode contact noise is caused due to loss of contact between the electrode and skin, which effectively makes disconnection for the measurement system from the subject. The loss of contact can be intermittent or can be permanent, as the case when a loose electrode is brought in and out of contact with the body skin of patient as a result of movements and vibration. This switching action can introduce large artefacts since the ECG signal is usually capacitively coupled to the system.

2.2.3 Motion Artifacts

Motion artefacts are transient baseline changes due to the variations in the electrode-skin impedance with electrode motion. The ECG amplifier exhibits different source impedance, and that forms a voltage divider with the amplifier input impedance. Therefore, the amplifier input voltage depends on the source impedance, which changes as the electrode position changes. The usual cause of motion artefacts is the movement or vibrations of the patient.

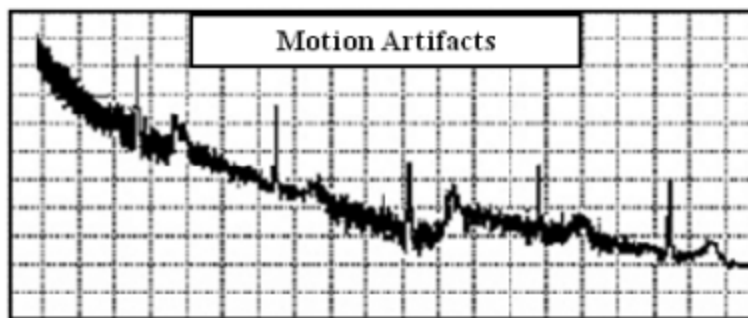


Fig 2.2 Motion Artifacts

2.2.4 Muscle Contractions

Muscle contractions cause artefact of millivolt-level to be generated . The baseline electromyogram is usually in the microvolt range and therefore is usually insignificant. The signals resulting from muscle contraction can be approximated to be transient bursts of band-limited Gaussian noise that interface and distort with ECG signal. The variance of the distribution may be estimated from the variance and duration of the bursts.

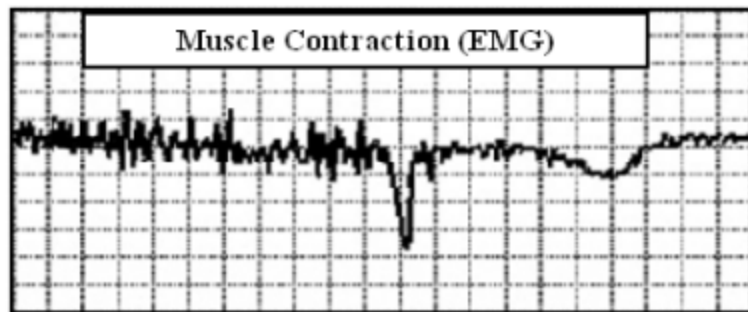


Fig 2.3 Muscle Contractions

2.2.5 Electrosurgical noise

Electrosurgical noise is caused by the electrosurgical instrument that uses to record ECG signal and operates on high voltages. During electrosurgical instrument activation, extraordinarily large transient voltages (100 - 400 V) are generated ubiquitously over the patient's skin surface. Electrosurgical noise completely destroys the ECG and can be represented by a large amplitude sinusoid with frequencies set approximately between 100 KHz and 1 MHz. While, the sampling rate of an ECG signal is 250 to 1000 Hz, an aliased version of this signal would be added to the ECG signal. The amplitude, duration, and possibly the aliased frequency should be variable.

2.2.6 Baseline drift noise

A significant wandering baseline in the ECG occurs due to variations in electrode-skin impedance. The main source of baseline wandering is respiration and the frequency ranges between 0.15 to 3 Hz. The baseline wander is an extraneous, low-frequency activity in the ECG which may interfere with the signal analysis, making the clinical interpretation inaccurate. When baseline wander takes place, ECG measurements related to the isoelectric line cannot be computed since it is not well-defined. Drift of the baseline can be represented as a sinusoidal component at the frequency of respiration added to the ECG signal.

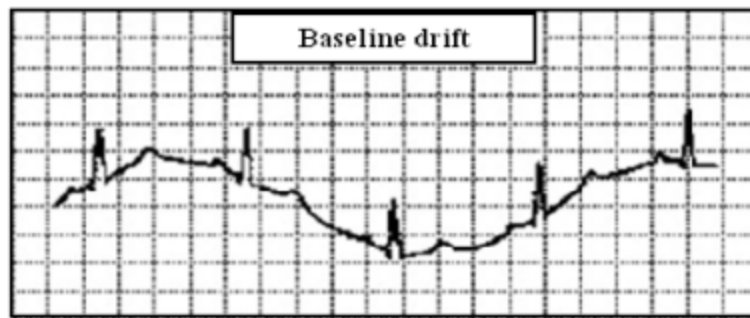


Fig 2.4 Baseline drift noise

Chapter 3

DWT Techniques in Signal Transforms

3.1 Wavelet transform filtering

Wavelet transform technique is another tool that can be used to analyse ECG signals by locating the interesting characteristic points to detect possible cardiovascular abnormalities. The problem is complicated, since most of the time the desired ECG signals are either corrupted or embedded in noises. Wavelet theory provides a unified framework for a number of techniques, which have been developed independently for various signal-processing applications. For example, multiresolution signal processing is used in computer vision; subband coding, developed for speech and image compression. Wavelet series expansions are developed using complex mathematics that implemented over recent years as a powerful time–frequency analysis and signal coding tool favoured for the interrogation of complex nonstationary signals. Wavelet treats both the continuous and the discrete time cases. It provides wide range of techniques that can be applied to accomplish tasks in signal processing, and therefore has numerous potential applications. In particular the "wavelet" transform (WT) is of interest for the analysis of non-stationary signals, because it provides an alternative to the classical STFT or Gabor transform. In contrast with the STFT, which uses a single analysis window, WT uses short windows at high frequencies and long windows at low frequencies . WT can also be viewed as signal decomposition tool that decomposes signal into a set of basic functions called “wavelets”. Those wavelets are obtained from a single mother wavelet that stretches and shifts according to the ECG signal.

Continuous Wavelet Transform (CWT) is defined as the sum of all time intervals that multiplied by scaled, shifted versions of the wavelet function or alternatively as shown in the following equation

$$\varphi(a, \tau) = \frac{1}{\sqrt{a}} \int s(t) \varphi\left(\frac{t-\tau}{a}\right) dt \text{----- (3.1)}$$

In this equation, the parameter is the scaling factor that stretches or compresses the function. Parameter is the translation factor that shifts the mother wavelet along the axis.

3.2 Application Of WT In Denoising

- **Medical Image / Signal Analysis.**
- **Data Mining.**
- **Radio Astronomy.**

Discrete wavelet transform (DWT), which transforms a discrete time signal to a discrete wavelet representation. It converts an input series x_0, x_1, \dots, x_m , into one high-pass wavelet coefficient series and one low-pass wavelet coefficient series (of length $n/2$ each) given by:

$$H_i = \sum_{m=0}^{k-1} x_{2i-m} \cdot s_m(z) \quad \text{---(3.2)}$$

$$L_i = \sum_{m=0}^{k-1} x_{2i-m} \cdot t_m(z) \quad \text{---(3.3)}$$

where $s_m(Z)$ and $t_m(Z)$ are called wavelet filters, K is the length of the filter, and $i=0, \dots, [n/2]-1$.

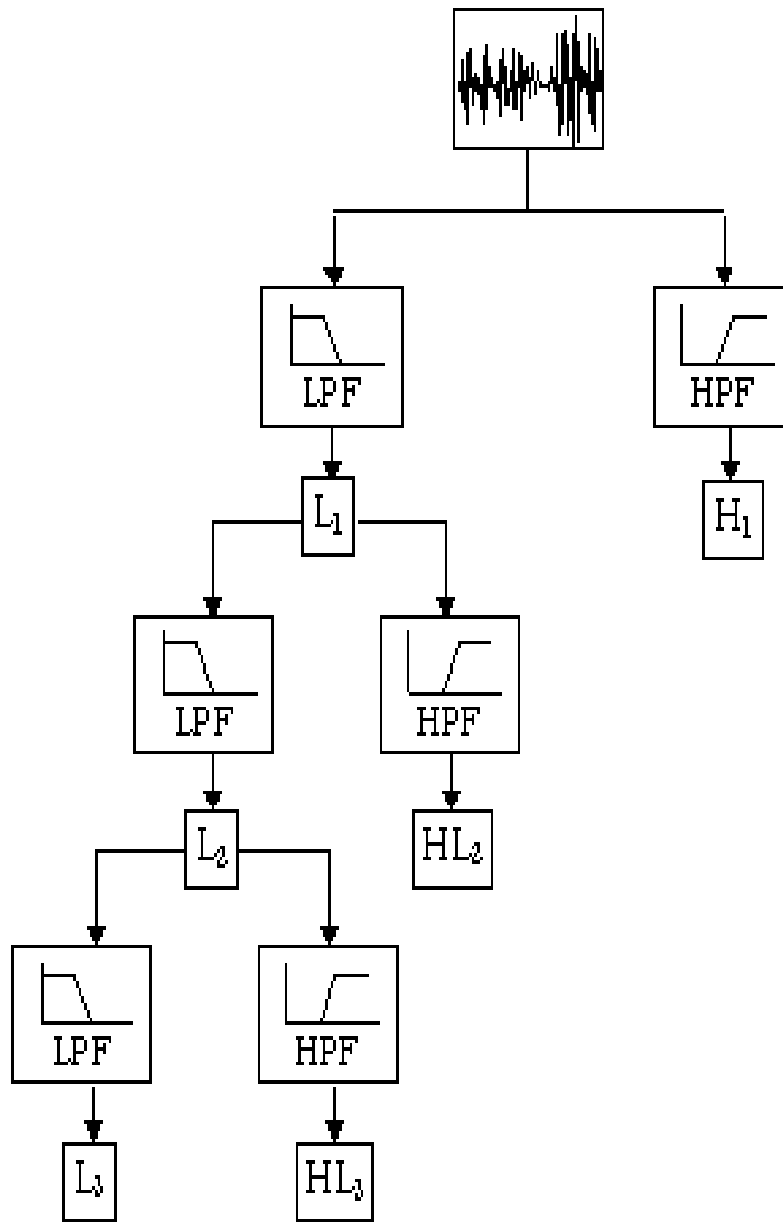


Fig 3.1 Continuous Wavelet Transform

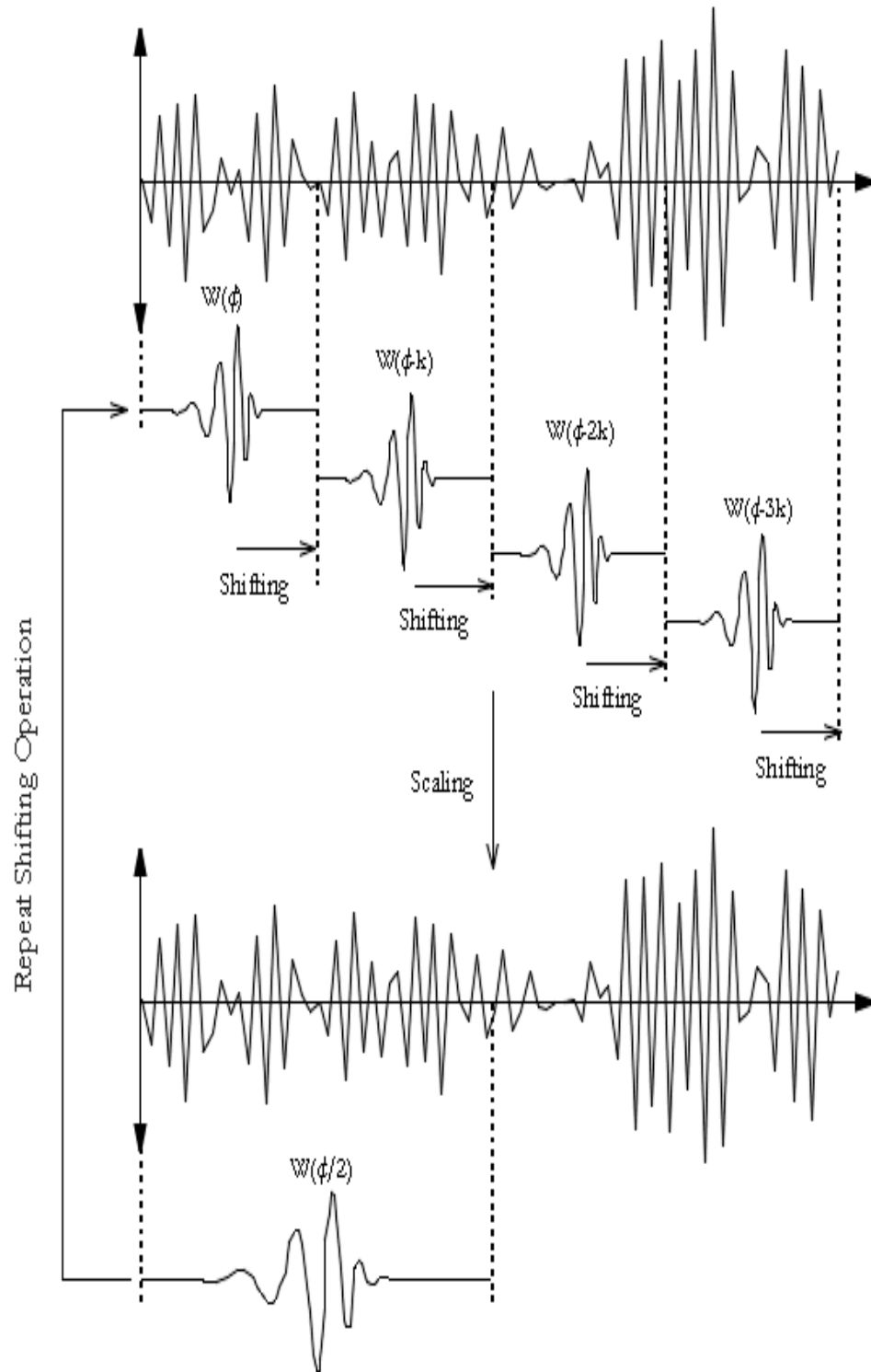


Fig 3.2 Repeat Shifting and Scaling of Wavelets in CWT

3.3 Types Of Wavelets

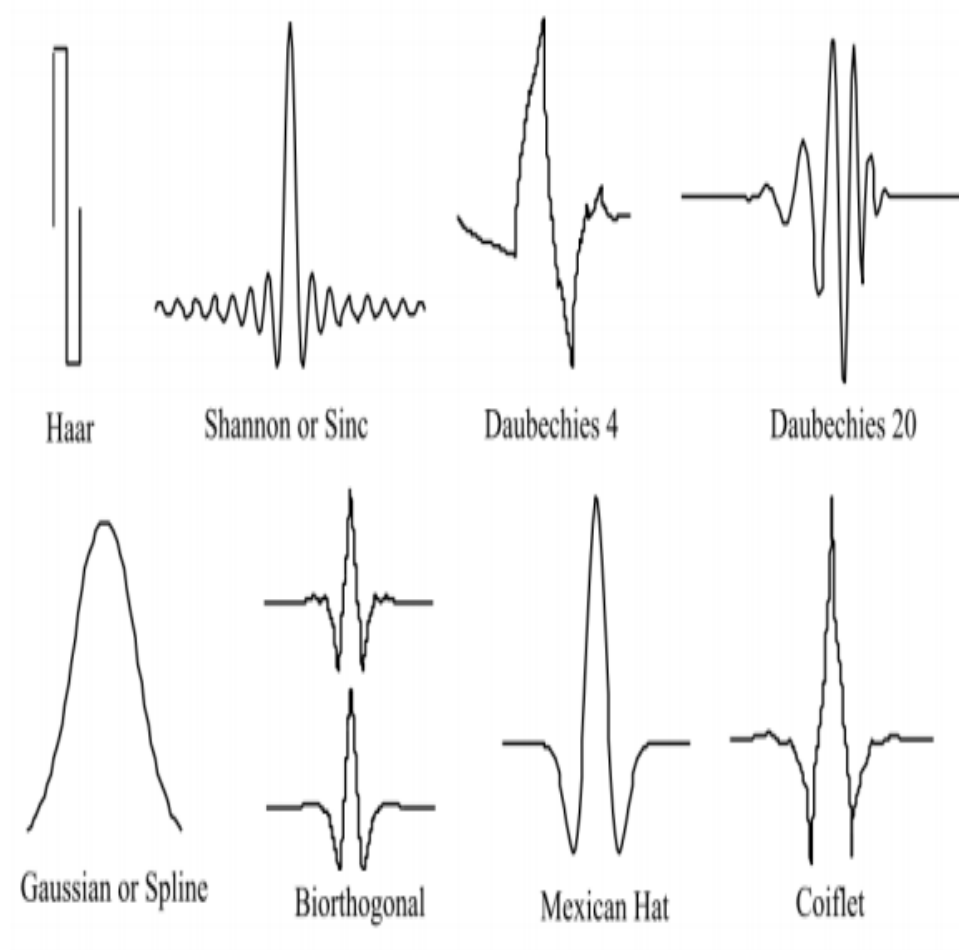


Fig 3.3 Types of Wavelets

3.4 Heart Rate monitoring

In current times the problems related to heart rate abnormalities have grown at a galloping speed and hence the needs for the proper and continuous monitoring of heart rate in heat patients and sportspersons have become inevitable and highly essential.

3.4.1 Normal Heart Rates

- Newborn- 120 To 160 Bpm.
- 1 To 5 Year- 100 To 140 Bpm.
- 6 To 15 Year- 80 To 120 Bpm.
- Adult And More - 60 To 100 Bpm

3.4.2 Heart Rate Disorders

- Tachycardia
- Bradycardia

3.4.3 Tachycardia

Tachycardia, is a heart rate that exceeds the normal resting rate. In general, a resting heart rate over 100 beats per minute is accepted as tachycardia in adults. Heart rates above the resting rate may be normal (such as with exercise) or abnormal (such as with electrical problems within the heart).

Physiological conditions when Tachycardia occurs are:

- Exercise
- Pregnancy
- Emotional conditions such as anxiety or stress.

Pathological conditions when Tachycardia occurs are:

- Sepsis
- Fever
- Anaemia

- Hypoxia
- Hyperthyroidism
- HyperSecretion of Catecholamines
- Cardiomyopathy
- Valvular Heart Diseases
- Acute Radiation Syndrome

General Heart Beat Levels for people suffering from Tachycardia at different ages

- Newborn > 160 Bpm.
- 1 To 5 Year > 140 Bpm.
- 6 To 15 Year > 120 Bpm.
- Adult And More > 100 Bpm.

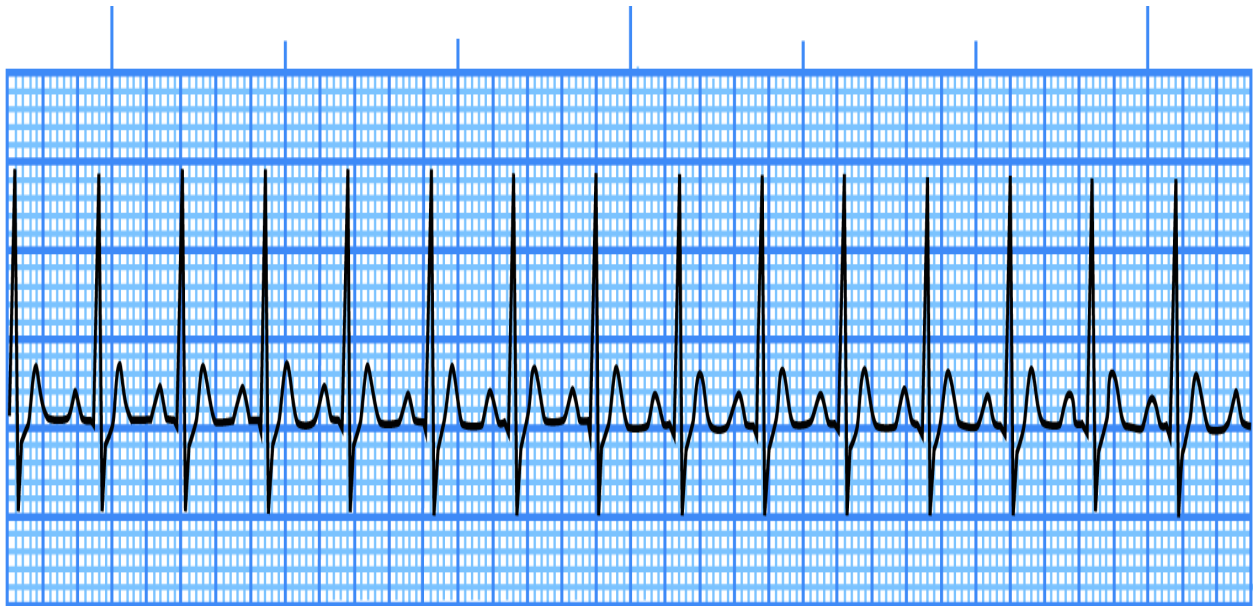


Fig 3.4 ECG Wave representing the condition Tachycardia

3.4.4 Bradycardia

Bradycardia, is a slow heart rate, defined as a heart rate of under 60 beats per minute(BPM) in adults. Bradycardia typically does not cause symptoms until the rate drops below 50 BPM. When symptomatic, it may cause fatigue, weakness, dizziness, and at very low rates, fainting.

Setting a lower threshold for Bradycardia prevents misclassification of fit individuals as having a pathologic heart rate. The normal heart rate number can vary as children and adolescents tend to have faster heart rates than average adults. Bradycardia may be associated with medical conditions such as hypothyroidism. Trained athletes tend to have slow resting heart rates, and resting Bradycardia in athletes should not be considered abnormal if the individual has no symptoms associated with it.

General Heart Beat Levels for people suffering from Bradycardia at different ages :

- Newborn < 120 Bpm.
- 1 To 5 Year < 100 Bpm.
- 6 To 15 Year < 80 Bpm.
- Adult And More < 60 Bpm.

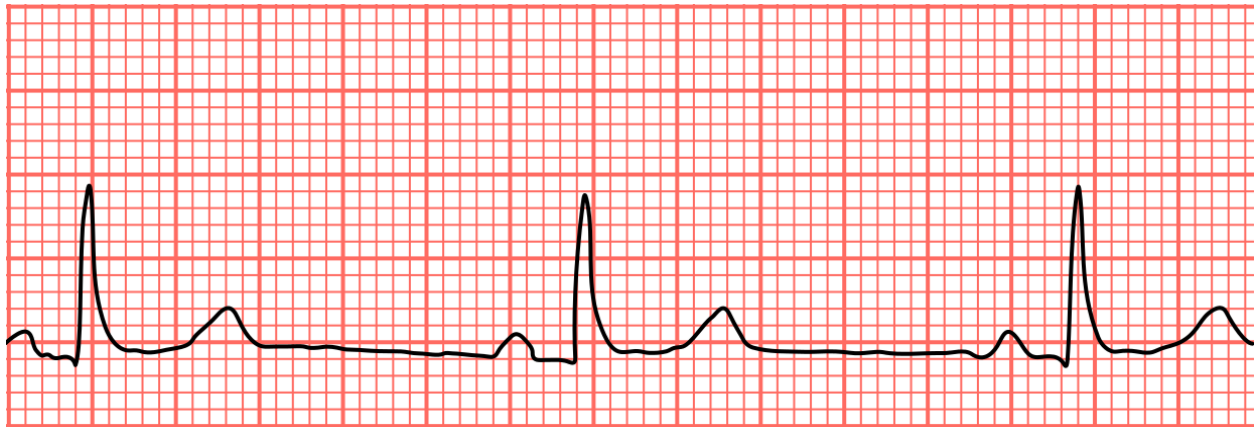


Fig 3.5 ECG Wave representing the condition Bradycardia

3.5 Determining the Heart Rate

- 15 Second Rule.
- RR Interval Rule.

3.5.1 15 Second Rule

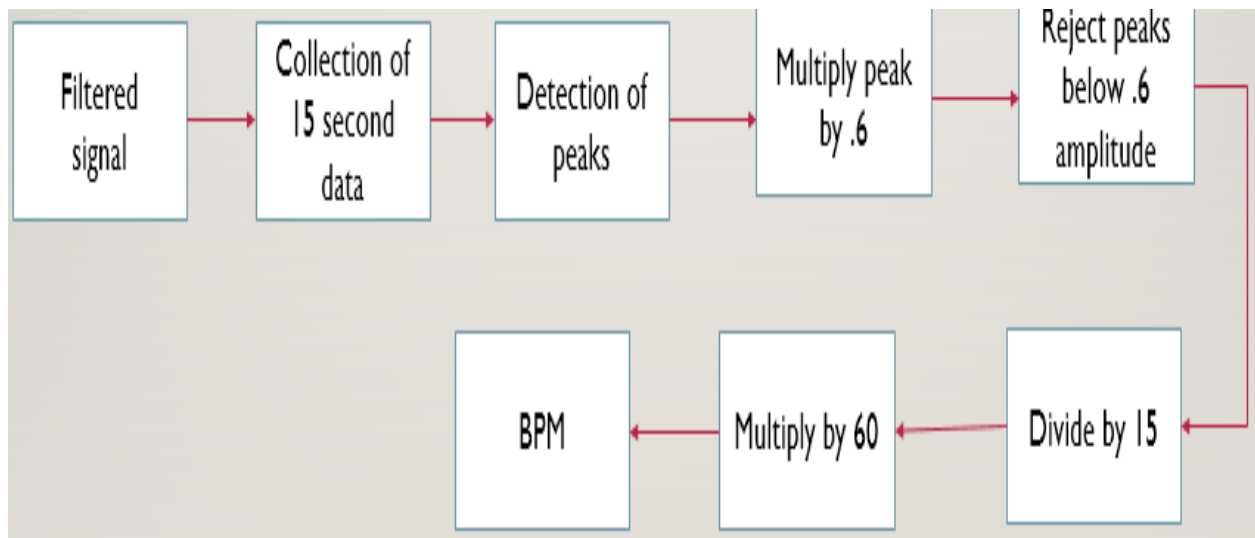


Fig 3.6 15 Second Rule Block Procedure Diagram

3.5.2 RR Interval Rule

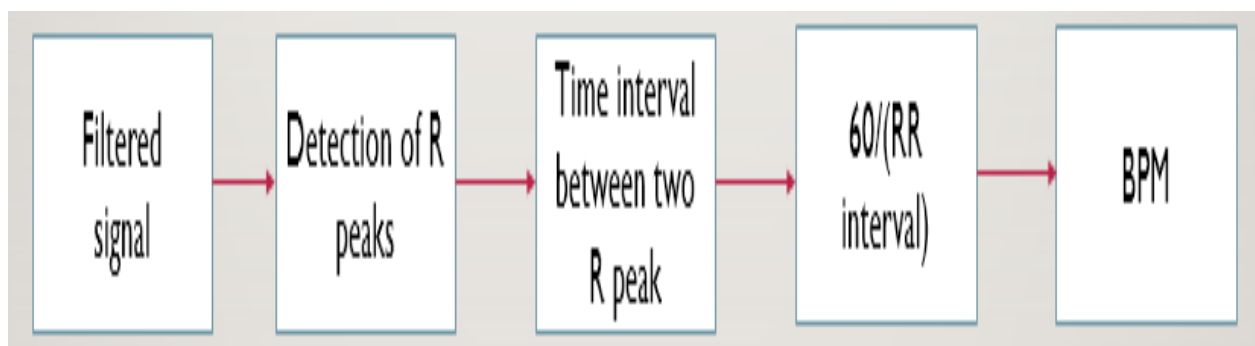


Fig 3.7 RR Interval Rule P3.5.2 RR Interval Rule procedure Block Diagram

3.6 QRS Complex detection

The “QRS complex” is the combination of the Q, R and S waves and represents ventricular depolarization in the heart atrium. This term can be confusing since not all ECG leads contain all three of these waves, yet a QRS complex does not have to contain a Q wave, but only R and S waves. Combination of R and S waves is still referred to as the QRS complex. The QRS duration will lengthen when electrical activity takes a long time to travel throughout the ventricular myocardium. The normal conduction system in the ventricles is called the His-Purkinje system and consists of cells that can conduct electricity quite rapidly as shown in Figure 3.1. The electrical impulse of normal conduction flows through the AV node then to the ventricles via the His-Purkinje system is causing a normal QRS duration. When electrical activity does not conduct through the His-Purkinje system, but instead travels from myocyte to myocyte to make QRS complex wider than P and T waves in time domain.

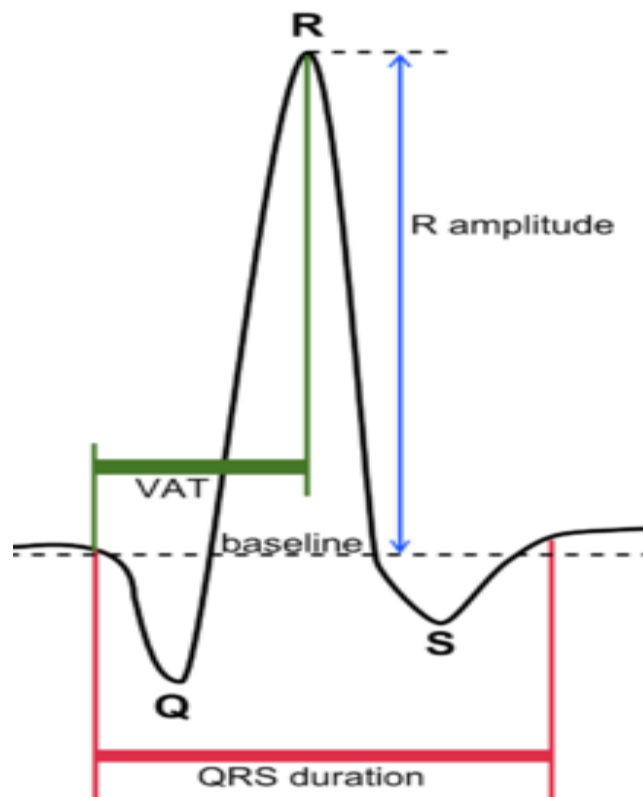


Fig 3.8 QRS Complex Waveform

3.7 The Pan-Tompkins Algorithm for QRS detection

Pan and Tompkins proposed a real-time QRS detection algorithm based on analysis of the slope, amplitude, and width of QRS complexes. The algorithm includes a series of filters and methods that perform low pass, high pass, derivative, squaring, integration, adaptive thresholding, and search procedures.

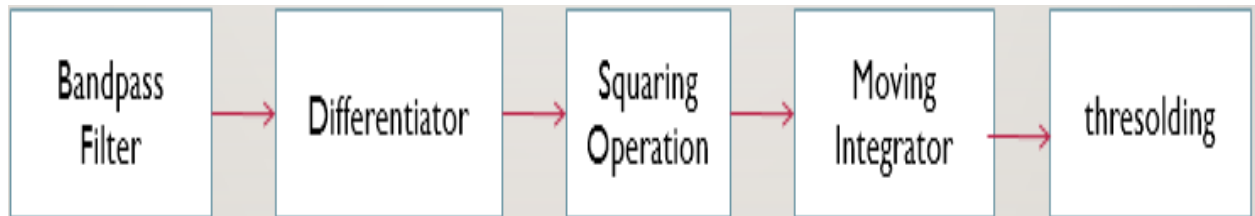


Fig 3.9 Block diagram of the Pan-Tompkins algorithm for QRS detection

3.7.1 Low Pass filter

The recursive lowpass filter used in the Pan-Tompkins algorithm has integer coefficients to reduce computational complexity, with the transfer function defined as

$$H(z) = \frac{1 (1 - z^{-6})^2}{32 (1 - z^{-6})^2} \text{----- (3.4)}$$

The output $y(n)$ is related to the input $x(n)$ as

$$y(n) = 2y(n-1) - y(n-2) + 1/32[x(n) + x(n-12) - 2x(n-6)] \text{----- (3.5)}$$

With the sampling rate being 200 Hz, the filter has a rather low cutoff frequency of $f_c = 11$ Hz, and introduces a delay of 5 samples or 25 ms. The filter provides an attenuation greater than 35 dB at 60 Hz, and effectively suppresses power-line interference, if present.

3.7.2 High Pass filter

The high pass filter used in the algorithm is implemented as an all pass filter minus a low pass filter.

$$H_{hp}(z) = z^{-16} - \frac{1}{32}H_{lp}(z) \text{-----} (3.6)$$

The output $p(n)$ of the high pass filter is given by the difference equation.

$$p(n) = x(n-16) - 1/32 [y(n-1) + x(n) - x(n-32)] \text{-----} (3.7)$$

The highpass filter has a cutoff frequency of 5 Hz and introduces a delay of 80 ms.

3.7.3 Derivative Operator

The derivative operation used by Pan and Tompkins is specified as

$$y(n) = 1/8 [2x(n) + x(n-1) - x(n-3) - 2x(n-4)] \text{-----} (3.10)$$

approximates the ideal d/dt operator up to 30 Hz. The derivative procedure suppresses the low-frequency components of the P and T waves, and provides a large gain to the high-frequency components arising from the high slopes of the QRS complex.

3.7.4 Squaring

The squaring operation makes the result positive and emphasizes large differences resulting from QRS complexes; the small differences arising from P and T waves are suppressed. The high-frequency components in the signal related to the QRS complex are further enhanced.

3.7.5 Integration

As observed in the previous subsection, the output of a derivative based operation will exhibit multiple peaks within the duration of a single QRS complex. The Pan-Tompkins algorithm performs smoothing of the output of the preceding operations through a moving-window integration filter as

$$y(n) = 1/N [x(n-(N-1)) + x(n-(N-2)) + \dots + x(n)] \text{-----} (3.11)$$

The choice of the window width N is to be made with the following considerations: too large a value will result in the outputs due to the QRS and T waves being merged, whereas too small a value could yield several peaks for a single QRS. A window width of $N = 30$ was found to be suitable for $f_b = 200$ Hz.

3.7.6 Adaptive thresholding

The thresholding procedure in the Pan-Tompkins algorithm adapts to changes in the ECG signal by computing running estimates of signal and noise peaks. A peak is said to be detected whenever the final output changes direction within a specified interval.

3.8 Derivative Based QRS detection

In a cardiac cycle, the QRS complex has the largest slope i.e. larger rate of change of voltage. This is due to the rapid conduction and depolarization characteristics of the ventricles. The derivative gives the rate of change. So in an attempt to develop an algorithm to detect the QRS complex the d/dt operation would be the most logical starting point.

There are various techniques like Pan-Tompkins model, bandpass filtering technique, template matching technique etc. that can be implemented to detect a QRS wave. Amongst them the differentiation technique is also an efficient technique detect the R peaks of a QRS complex. The basis of many detection techniques is differentiation. It is basically a high pass filter. Whenever the derivative of a signal is taken the higher frequencies characteristic of the QRS complex gets amplified while attenuating the lower frequencies of the P and T wave . An algorithm based on the first order, second order and third order derivative has been used to detect the peaks. The figures below shows the steps involved in the signal processing.

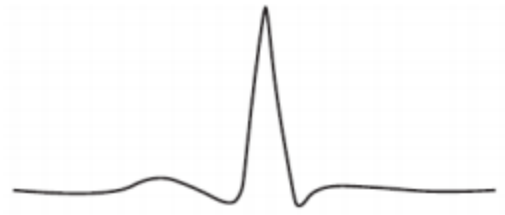


Fig 3.12 Original ecg signal



Fig 3.13 First order derivative having a smooth and rectified signal

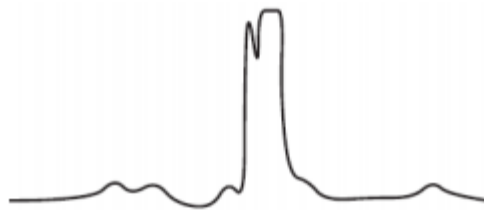


Fig 3.14 Second Order Derivative having a smooth and rectified signal

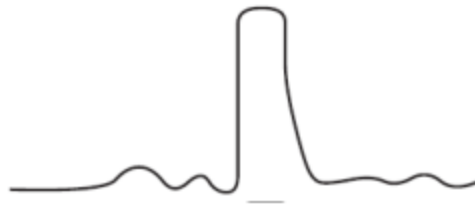


Fig 3.15 Sum of First and Second Order Derivative



Fig 3.16 Square Pulse Output for each QRS complex

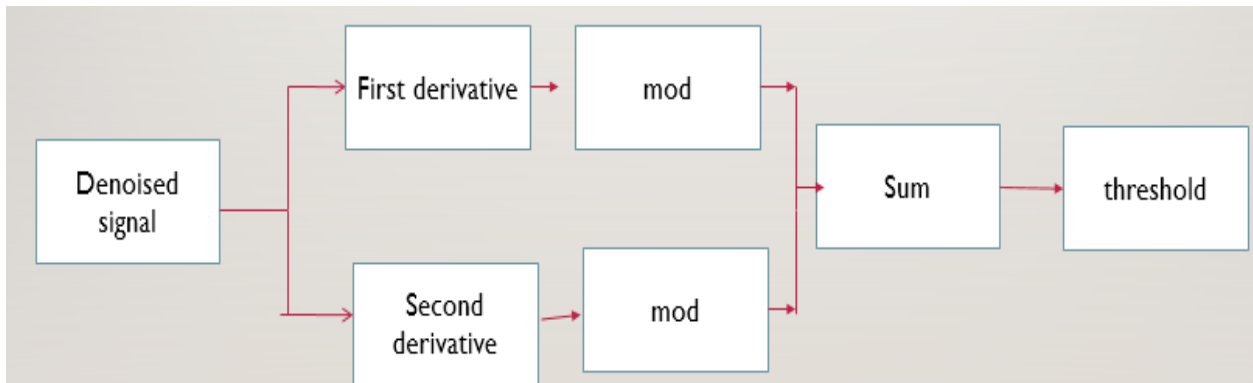


Fig 3.17 Block Diagram of Denoising and Thresholding of Waveform.

$$y_0(n) = |x(n) - x(n-2)| \text{-----}(3.7)$$

Second derivative is approximated as

$$y_1(n) = |x(n) - 2x(n-2) + x(n-4)| \text{-----}(3.8)$$

Two results are weighted and combined to obtain

$$y_2(n) = 1.3y_0(n) + 1.1y_1(n) \text{-----}(3.9)$$

- The result $y_2(n)$ is scanned with a threshold of 1.0. Whenever the threshold is crossed, the subsequent eight samples are also tested against the same threshold.
- If at least six of the eight points pass the threshold test, the segment of eight samples is taken to be a part of a QRS complex.
- The procedure results in a pulse with its width proportional to that of the QRS complex.

3.9 Multiscale Mathematical Morphology

Mathematical morphology was initiated in the late 1960s by G. Matheron and J. Serra, who found applications in anFig. Second Order Derivative having a smooth and rectified signalyzing images from geological or biological specimens.

It becomes one of the favorable signal analysis tools in many shape-oriented problems due to its rich theoretical framework, low computational complexity, and simple hardware implementation. The uniqueness of mathematical morphology is that it does not requires any prior knowledge on the frequency spectrum of the signal under investigation. For ECG signal processing, this feature brings the benefit of avoiding the frequency band overlapping of QRS complexes and other components, such as P/T waves.

Mathematical morphology is a powerful methodology for the quantitative analysis of geometrical structures. It consists of a broad and coherent collection of theoretical concepts, non linear signal operators, and algorithms aiming to extract information related to the shape and size from images or other geometrical objects . It provides a way to analyze signals by using nonlinear signal-processing operators. These operators serve two purposes (i.e., extracting the useful signal and removing the artifacts).

3.9.1 Mathematical Morphology

3M is an extension of the single-scale morphology (1M). Both of them share the same basic mathematical morphological operators: dilation, erosion, opening, and closing. The top-hat and bottom-hat operators are composite operations of those from before. The difference between 1M and 3M is that the latter applies morphological operators to the signal repeatedly by varying the shape and size of structure elements. The elementary single-scale mathematical morphology operators for length N signal $F(n)$ are listed below for reference, i.e., where indicates the th element in a length structure element, and is a predefined structure element.

$$\text{Dilation : } f \oplus g(n) = \max_{(i)} (f(n-i) + g(i))$$

$$\text{Erosion : } f \ominus g(n) = \min_{(i)} (f(n-i) + g(i))$$

$$\text{Opening : } f \circ g(n) = f \oplus g(\ominus g)(n)$$

$$\text{Closing : } f * g(n) = f \ominus g(\oplus g)(n)$$

$$\text{Top Hat : } \text{That}(f(n)) = f(n) - f \circ g(n)$$

$$\text{Bottom Hat : } \text{Bhat}(f(n)) = f(n) - f * g(n)$$

3.9.2 Implementation Schemes

QRS complexes are composed of a group of consecutive positive and negative peaks. 3M filtering plays the most critical role in the proposed algorithm which removes the noise in the ECG signal. Differential operation and multiple-frame accumulation further enhance the signal leading to accurate QRS detection.

A morphological operation is actually the interaction of a set or function representing the object or shape of interest with another set or function of simpler shape called structuring element. The shape of the structuring element determines the shape information of the signal that is extracted under such an operation. Two other operations are derived from the basic ones, opening and closing. Opening and closing offer an intuitively simple and mathematically formal way for peak or valley extraction.

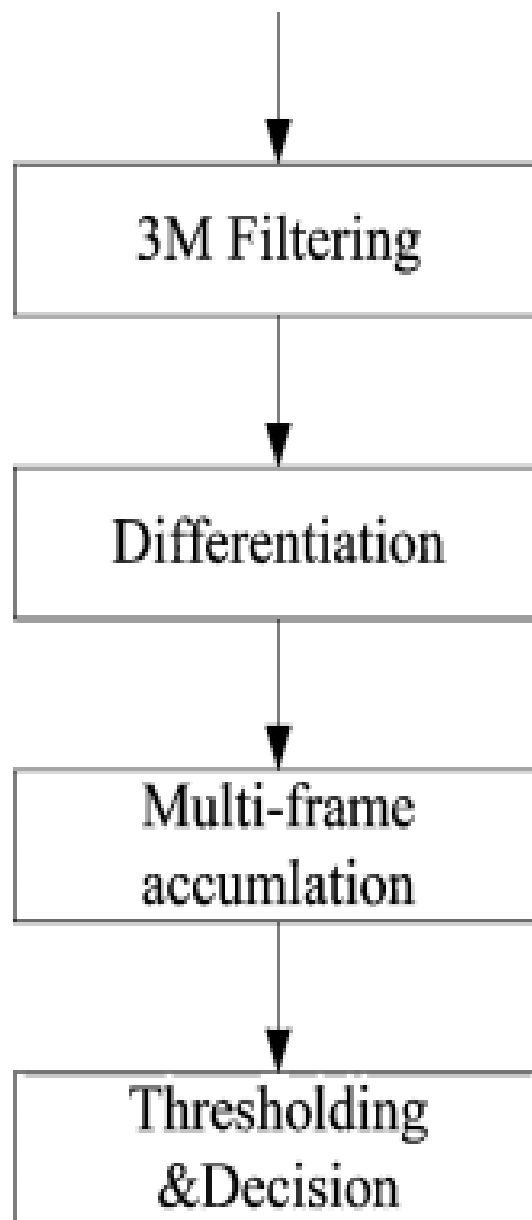


Fig 3.18 Block diagram of the proposed QRS detection algorithm.

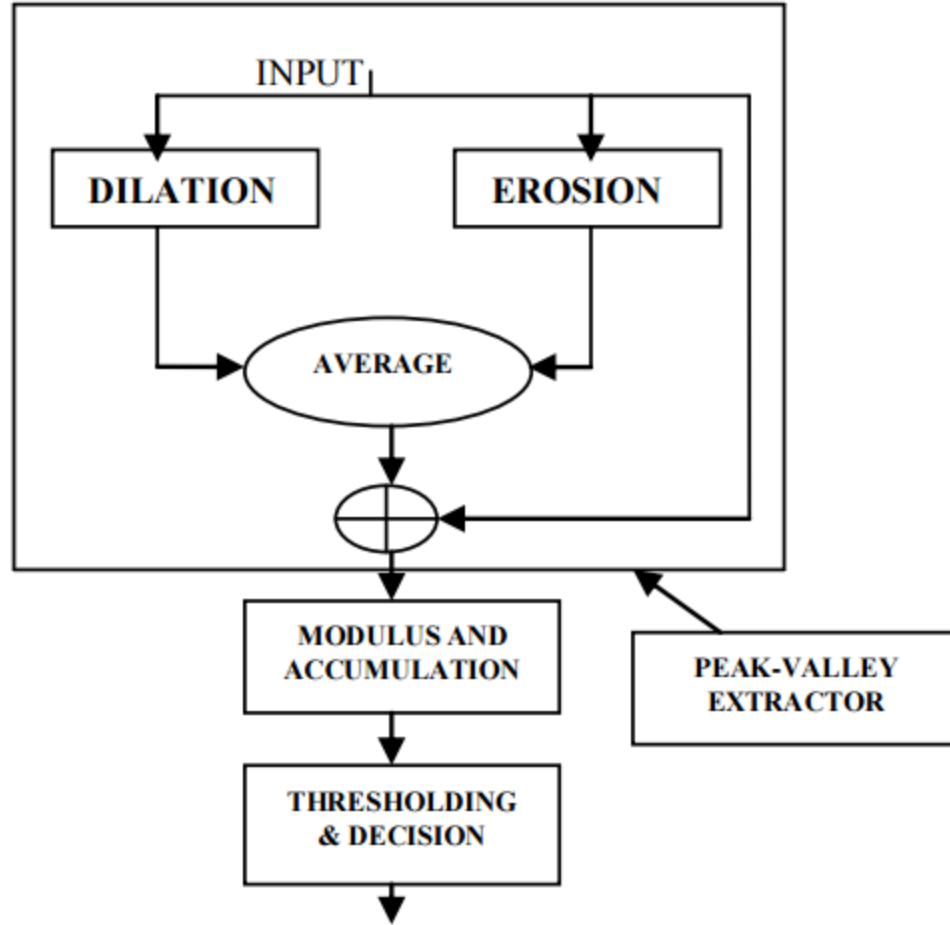


Fig 3.19 Removing baseline wandering module

3.9.3 Differential Operation

After 3M filtering, the output ECG sequence $y(n)$ is differentiated in order to remove motion artifacts and baseline drifts. The first-order derivative can be found by

$$v(n) = 1/\Delta(y(n) - y(n-1)) \text{-----}(3.11)$$

Where n indicates the current sample and $1/\Delta t$ is the sampling frequency.

3.9.4 Modulus operation

The absolute value of the differential output is combined by multiple-frame accumulation, which is very similar to energy transformation. The process is expressed as

$$s(n) = \sum_{i=n-[q/2]}^{n+[q/2]} |v(i)| \text{-----} (3.12)$$

The value of q should correspond to the possible maximum duration of the normal QRS complex.

3.10 Threshold and Decision

The detection of a QRS complex is accomplished by comparing the feature against a threshold. This threshold is used as the decision function in connection with the proposed transformation for QRS detection. Usually, the threshold levels are computed to be signal dependent such that an adaptation to changing signal characteristics is possible.

Selecting the threshold T is given by

$$T = \{0.1Max \text{ } Max < 3\}$$

$$T = \{0.27Max \text{ } 3 \leq Max \leq 5\}$$

$$T = \{0.15Max \text{ } Max > 5\}$$

3.11 ECG Feature Extraction

3.11.1 Windowing Algorithm

- Windowing method is used detect ECG timing intervals like the PR interval, QRS duration, the QT interval, the QT corrected interval and Vent Rate.
- Windows are based on varying R-R intervals.

3.12 Algorithm Proposed

- FIR Filter is used to remove the noises in the signal.
- DWT Technique is used to clean the signal and remove the noises completely.

- The cleaned signal is passed through Windowing Filter to detect R peaks and extract features.
- Extracted feature is used as a feature to predict Arrhythmia conditions.

3.13 Results

- **Plot of a Normal Heartbeat ECG waveform before signal processing and denoising**

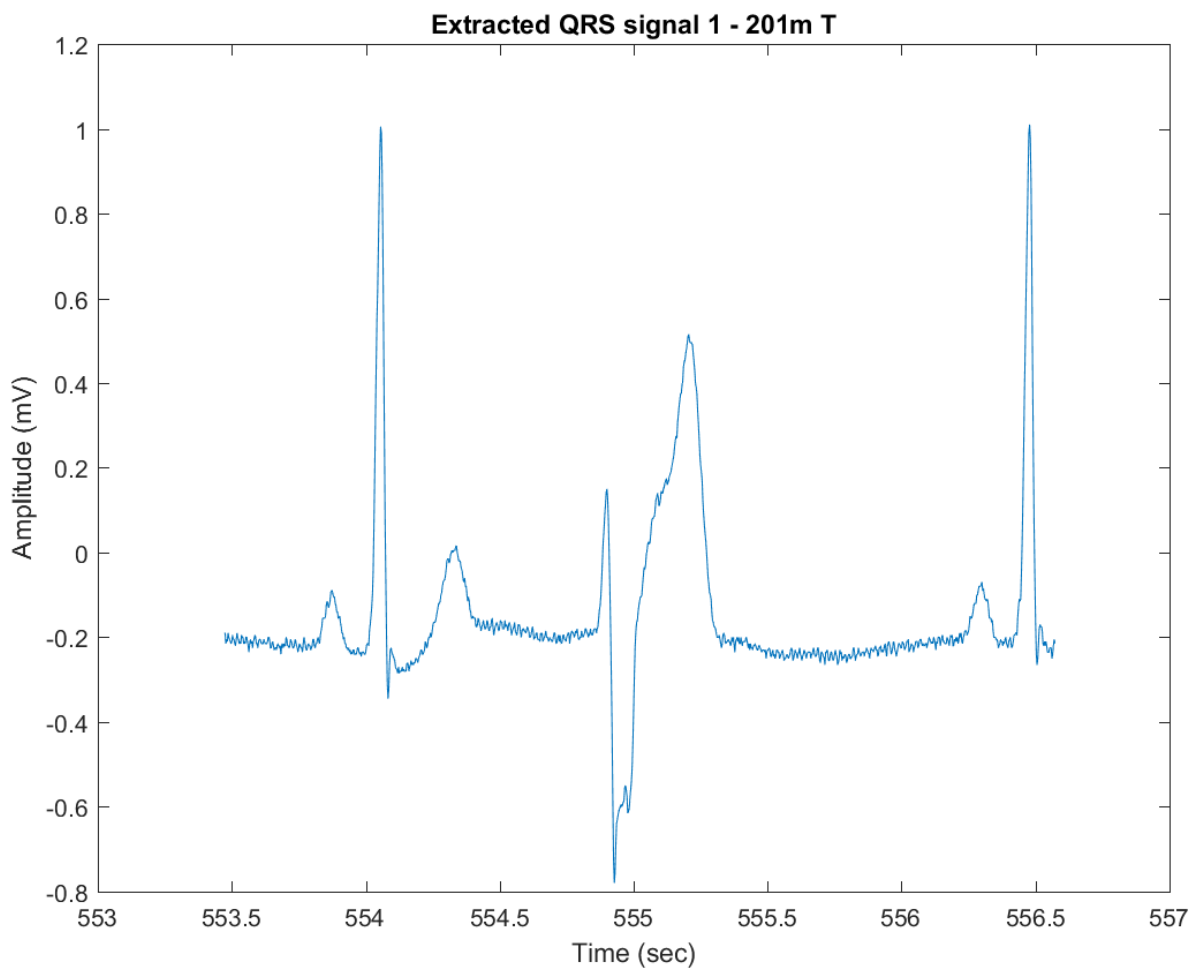


Fig 3.20 Plot Of ECG Waveform consisting QRS Complex

- **Plot of a denoised and processed ECG Signal with R Peaks detected using DWT Technique**

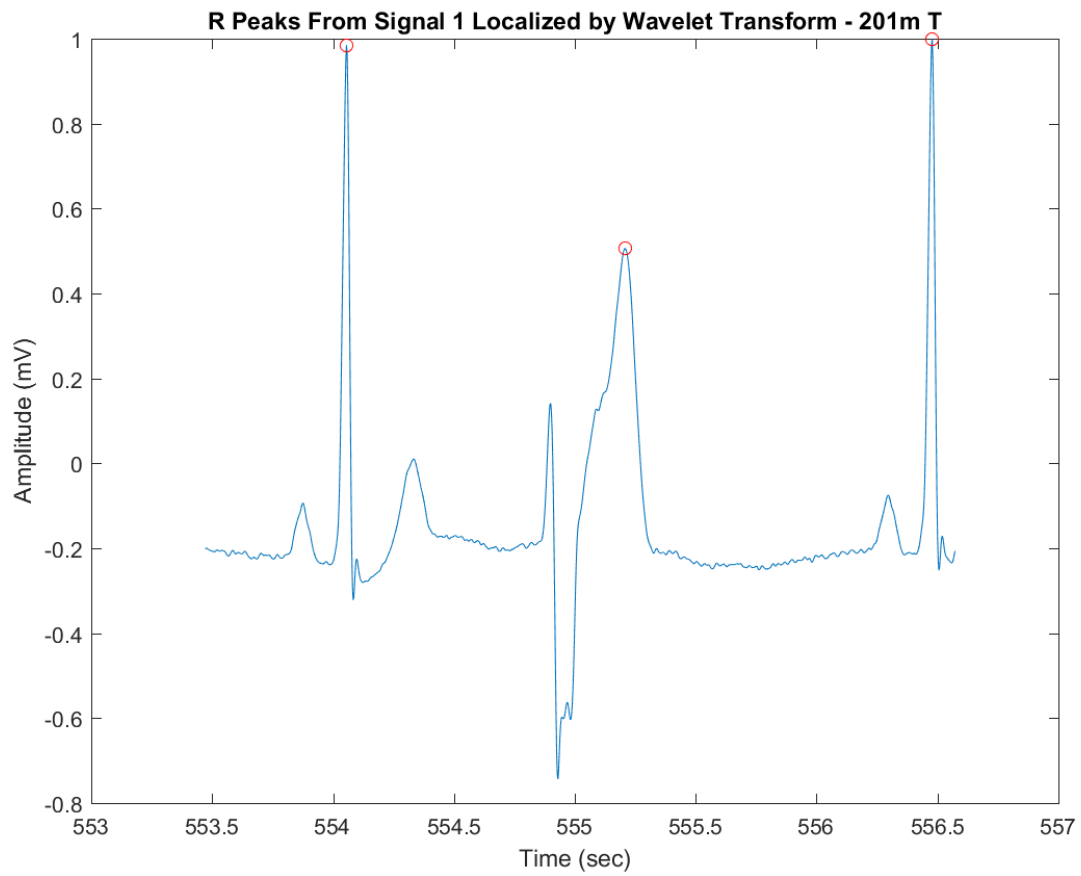


Fig 3.21 R Peaks Detected after using DWT Technique and denoising the ECG Signal.

Chapter 4

FFT Techniques in Signal Processing

4.1 Fast Fourier Transform

A fast Fourier transform (FFT) is a technique that solves the discrete Fourier transform (DFT) of a sequence, or its inverse (IDFT). Fourier analysis, firstly converts any given signal from its given domain mostly time to the frequency domain and vice versa. Generally, DFT is calculated by splitting sequence of values into components of different frequencies DFT is used in many fields of science and technology, but computing it directly from its definition is very slow and not practical. FFT is useful in this case it computes such transformations very fast by factorising the DFT matrix into a product of sparse factors. So in such a manner, FFT reduce the time complexity of DFT from $O(n^2)$ to $O(n \log n)$ by using FFT. The difference in speed can be very significant, especially for long data sets where N may be in the thousands or millions. In case of round-off error, FFT techniques are much more accurate than DFT techniques. There are many types of FFT techniques based on many theories, from simple complex-number arithmetic to group theory and number theory.

The best-known FFT techniques depend upon the factorization of N , but there are FFTs with $O(N \log N)$ complexity for all N , even for prime N . Many FFT techniques basically depend upon on $e^{(-2\pi i/N)}$ is an N th primitive root of unity, and thus can be applied to analogous transforms over any finite field, such as number-theoretic transforms. Basically the inverse DFT is the same as the DFT, but with only the sign difference in the exponent and a $1/N$ factor, any FFT technique can easily be adapted for it.

Let x_0, \dots, x_{N-1} be complex numbers. The DFT is obtained by the formula

$$X_k = \sum_{n=0}^{N-1} x_n e^{-i2\pi kn/N} \quad k = 0, 1, \dots, N-1 \quad \text{-----}(4.1)$$

where $e^{i2\pi/N}$ is a primitive Nth root of 1.

Calculating by this definition results in time complexity of $O(N^2)$: there are N outputs X_k , and each output requires a sum of N terms. FFT is used to get the same results in time complexity of $O(N \log N)$. All known FFT algorithms require $O(N \log N)$ operations, although there is no known proof that a lower time complexities can be possible.

To demonstrate the effectiveness of an FFT, consider the count of complex multiplications and additions for $N=1024$ data points. Evaluating the DFT's sums takes N^2 complex multiplications and $N(N-1)$ complex additions, of which $O(n)$ operations can be saved by eliminating trivial operations such as multiplications by 1, leaving about 30 million operations. On the other hand, the radix-2 Cooley–Tukey algorithm, for N a power of 2, can compute the same result with only $(N/2)\log_2(N)$ complex multiplications (again, ignoring simplifications of multiplications by 1 and similar) and $N \log_2(N)$ complex additions, in total about 30,000 operations - a thousand times less than with direct evaluation. In practice, actual performance on modern computers is usually dominated by factors other than the speed of arithmetic operations and the analysis is a complicated subject, but the overall improvement from $O(n^2)$ to $O(n \log n)$ remains.

The most commonly used FFT is the Cooley–Tukey algorithm. This is basically a divide and conquer algorithm that repeatedly breaks down a DFT of any size $N = N_1 N_2$ into many smaller DFTs of sizes N_1 and N_2 , along with $O(N)$ multiplications by complex roots of unity traditionally called twiddle factors.

The best known use of the Cooley–Tukey algorithm is to divide the transform into two pieces of size $N/2$ at each step, and is therefore limited to power-of-two sizes, but any factorization can be used in general (as was known to both Gauss and Cooley/Tukey). These are called the radix-2 and mixed-radix cases, respectively (and other variants such as the split-radix FFT have their own names as well). Although the basic idea is recursive, most traditional implementations rearrange the algorithm to avoid explicit recursion. Also, because the Cooley–Tukey algorithm breaks the DFT into smaller DFTs, it can be combined arbitrarily with any other algorithm for the DFT.

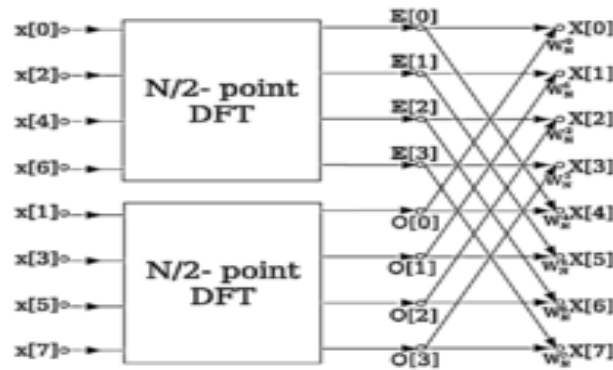


Fig 4.1 An example FFT algorithm structure, using a decomposition into half-size FFTs

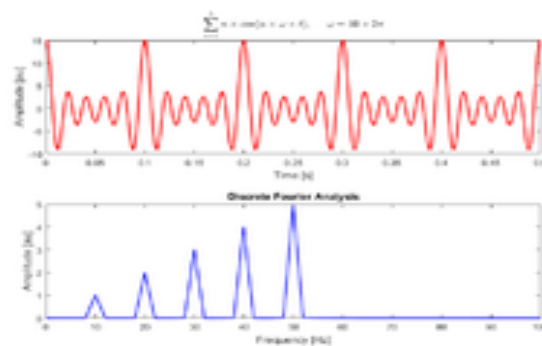


Fig 4.2 A discrete Fourier analysis of a sum of cosine waves at 10, 20, 30, 40, and 50 Hz

This FFT technique is used in our ECG signal processing. Basically, the obtained original ECG signal has many noise components due to various reasons of different frequencies. These noise components are of low frequencies. So, we use frequency domain to remove the low frequency noise components. Time domain is not used here as it plots the variation of signals with respective time, whereas in frequency domain the amplitude of the signals with respective frequencies are plotted which makes the job easy for our analysis.

The ECG Signals which are in time domain are converted to frequency domain by using FFT technique. We use FFT or DFT as computations are less and efficiency is more. After splitting into various frequency components a FIR(Finite Impulse Response) filter is used to eliminate the

lower frequency components. After filtering , now inverse FFT technique is used to get back the signal in time domain. FIR filter is can only be used in frequency domain but not in time domain. Our interest only rests in detecting the R peaks in ECG signal rather than the shape of the waveform so the technique can be implemented using the filters also.

After using the FFT technique the above waveform is obtained but we restrict it to detecting R peaks rather than on the entire waveform. So for this we use windowing filter

4.2 Windowing Filter

A windowing filter takes a definite sized window as input. The window can be of any shape and size but for our purpose we take a rectangular shaped window whose size can be adjusted and given as input to the filter this filter finds only the local maxima that observes only maximum in the window and ignores the other values.

Basically, it performs the spectral analysis of non periodic signals. The result obtained from this filter does not assure that it contains all peaks in all cases. We overcome the above disadvantage by repeating the window filter again and again with different window sizes . With altered window size R peaks inside different windows can be realised which were left unrealised when only a window of single size is used.

This thresholding filter is applied many times for accurately detecting the significant peaks.

In the Fig 4.5, many peaks are detected but all the peaks are not R peaks if we use this detected peaks in calculating the heart beat then we might get a wrong value so to avoid this ,the peaks of comparatively lower value than the threshold value are eliminated to do this we use Threshold Filter to remove the small peaks and keep the significant ones.

So to do this after the step of Windowing Filter we apply the Threshold Filter . Here, we take the threshold value as the minimum value to of the peak to be qualified as the R peak. Here in our case the amplitude of other segments (U, S, and T) should be less than one-third of R signal.

So by setting the threshold value, the threshold filter is applied to remove the small peaks and preserve the significant ones.

4.3 Calculation Of Heartbeat

After detecting all the R peaks the next important step is calculation of the heartbeat. The heart rate can be (beats/s) calculated by the formula

$$\text{Rate} = 60 * \text{Sampling rate} / (\text{R-R interval}) \text{----- (4.2)}$$

After calculation of the heart rate, heartbeat rate can be classified into 3 types.

They are:

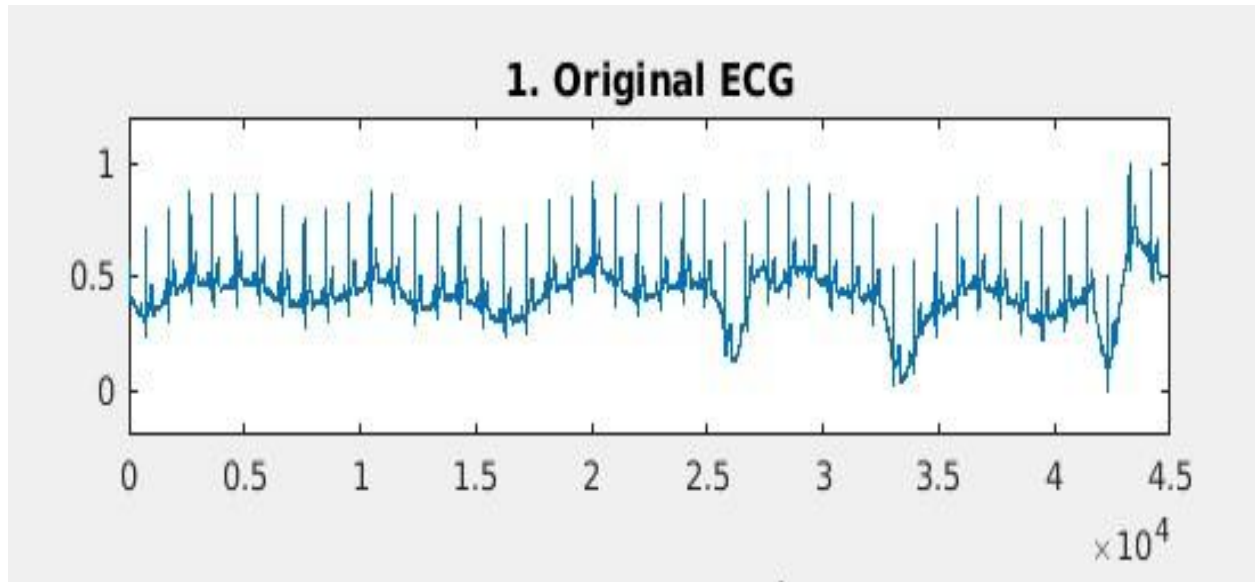
1. Heart beat < 60 , this is called BradyCardia (this occurs if patient might be suffering from Jaundice or Intra cardinal pressure)
2. Heart beat > 100, this is called TachyCardia (this occurs if patient might be suffering from high BP or nose bleeding)
3. Heart beat > 60 and < 100, usually this is normal heart beat rate

So in this way we detect the heartbeat and draw conclusions from it. But, there are many number of symptoms and there is particular type of heartbeat rhythm for a particular symptom. So, for accurately predicting the condition of the heart we use Machine Learning techniques.

4.4 Algorithm Proposed

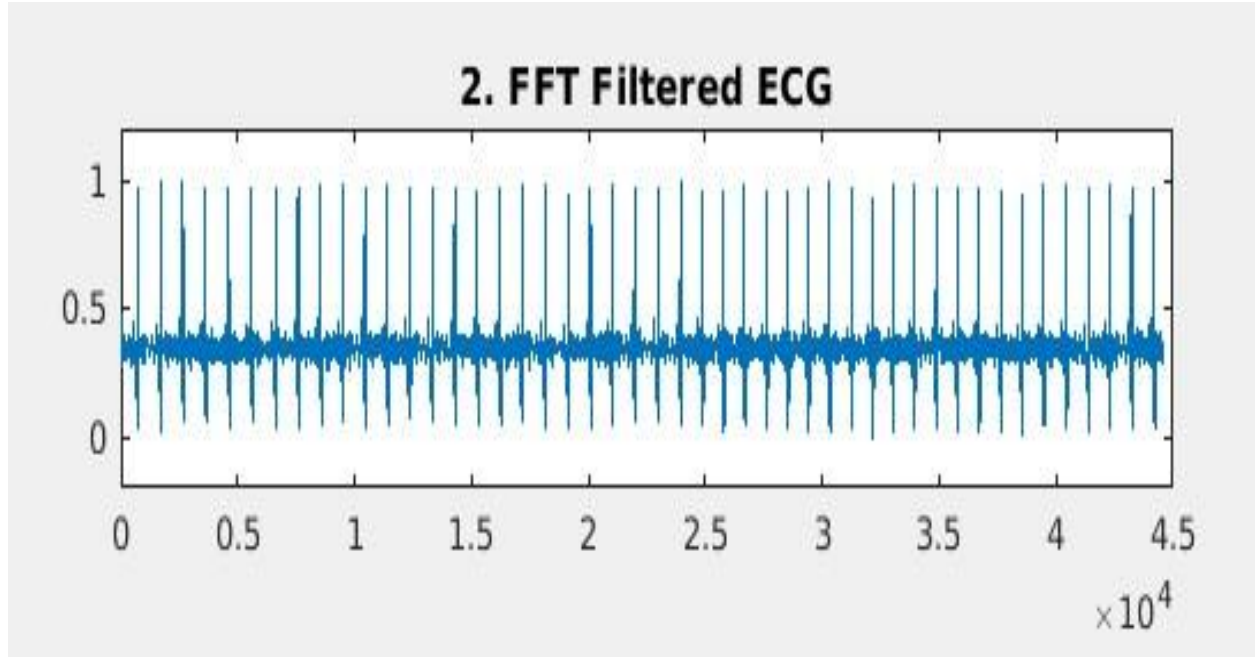
- FFT analysis is applied to remove lower frequency components
- After removing lower frequency IFFT is applied on the data.
- Windowing filter of a definite size (avg heart beat cycle) is used to detect peaks.
- Filtering the Signal to remove noise.
- Windowing filter of another size (greater than avg heart beat cycle) is used to detect peaks.
- Detected R peaks is used as a feature to predict the Arrhythmia condition.

4.5 Results



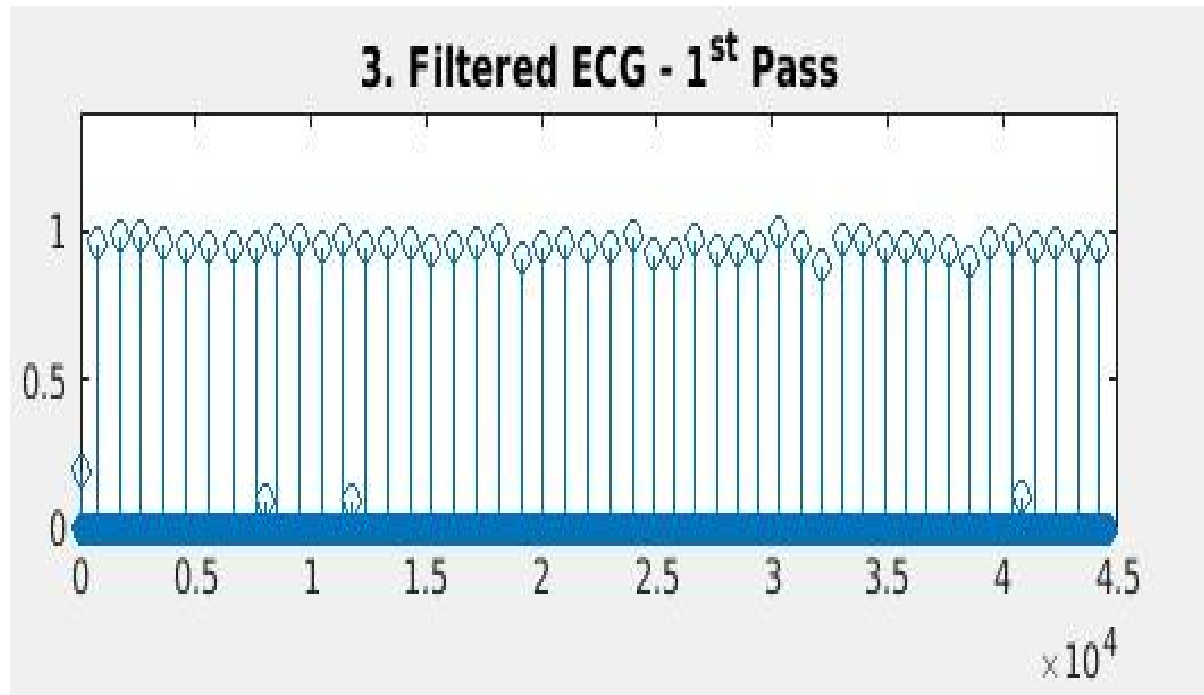
Y-Axis Represents the Amplitude of the signal and X-Axis Represents the Data Points.

Fig 4.3 Original ECG Signal Plotted



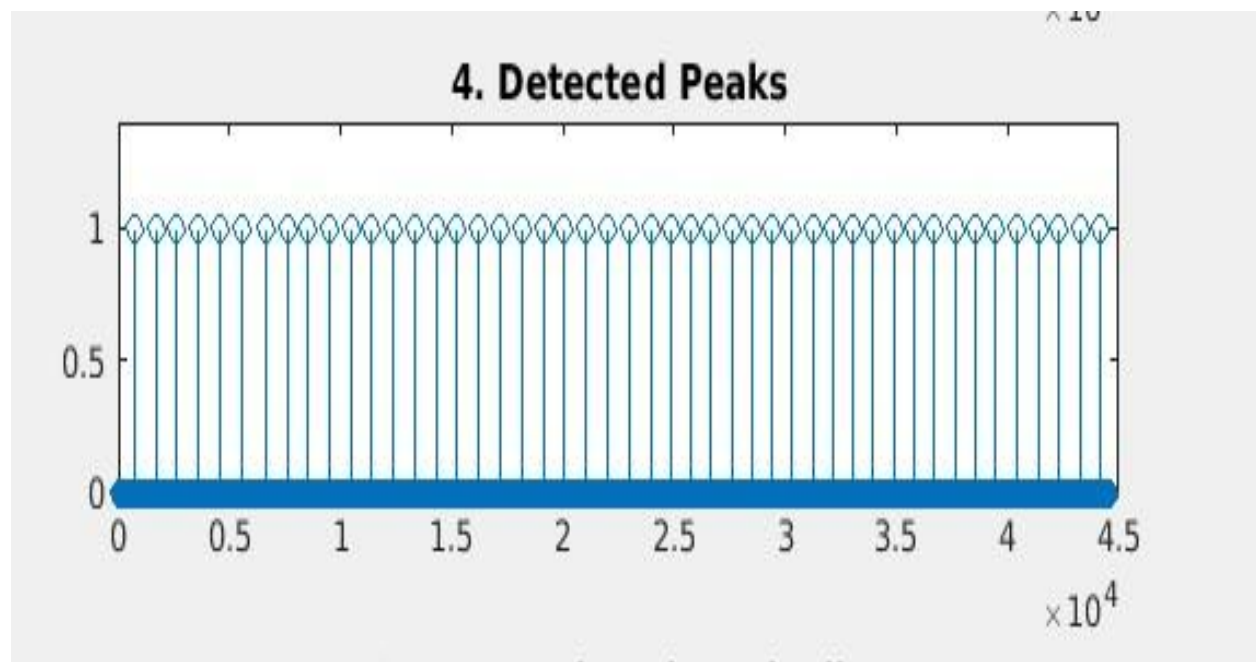
Y-Axis Represents the Amplitude of the signal and X-Axis Represents the Data Points.

Fig 4.4 FFT filtered ECG Signal.



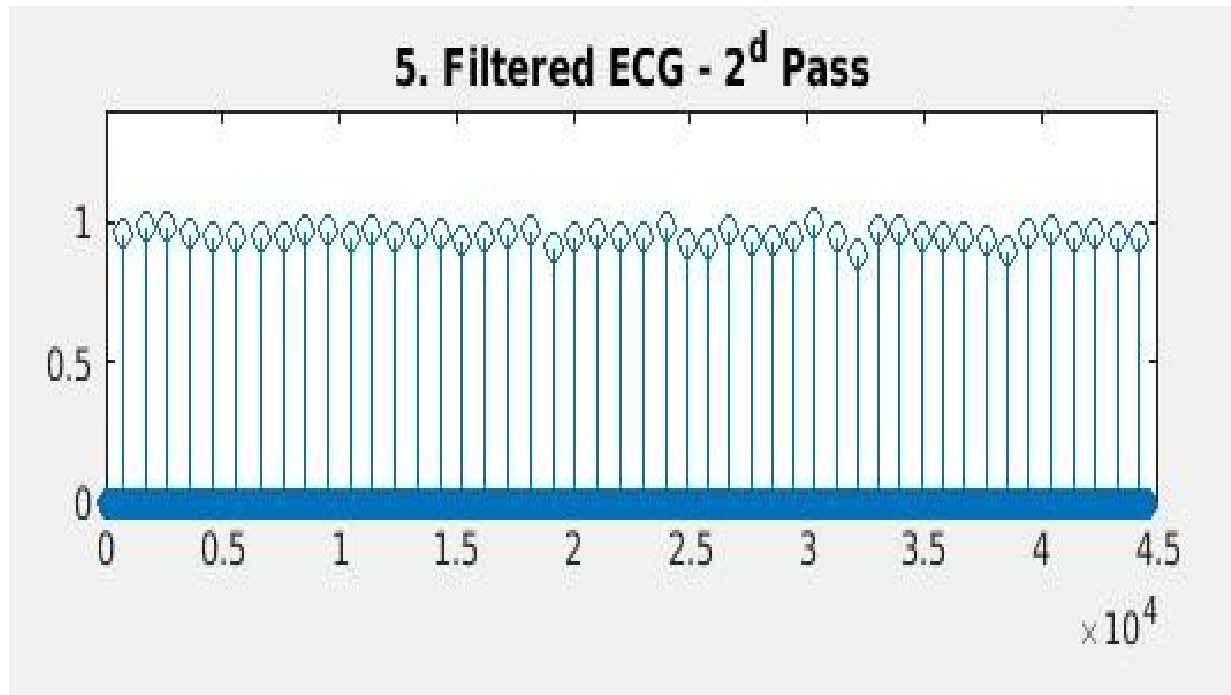
Y-Axis Represents the Amplitude of the signal and X-Axis Represents the Data Points.

Fig 4.5 Window Filtered ECG Signal (1st time)



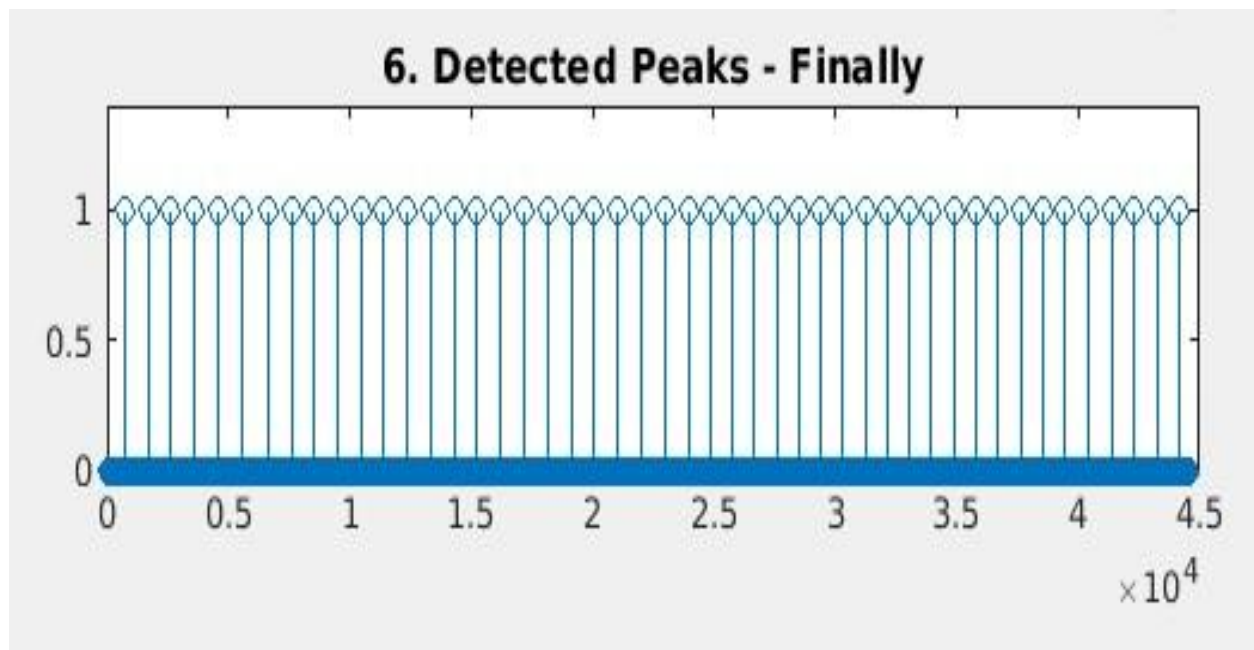
Y-Axis Represents the Amplitude of the signal and X-Axis Represents the Data Points.

Fig 4.6 Detected peaks after applying the threshold filter



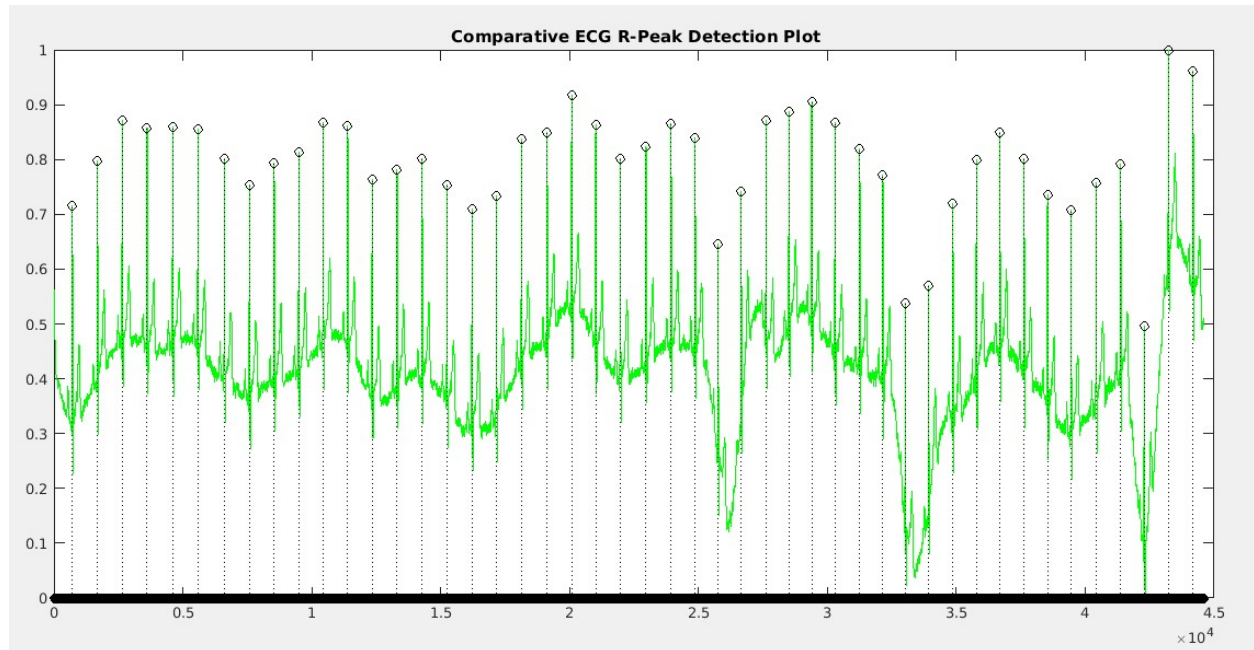
Y-Axis Represents the Amplitude of the signal and X-Axis Represents the Data Points.

Fig 4.7 Window Filtered ECG Signal (2nd time with different window size)



Y-Axis Represents the Amplitude of the signal and X-Axis Represents the Data Points.

Fig 4.8 Detected Peaks after passing through two different window filters.



Y-Axis Represents the Amplitude of the signal and X-Axis Represents the Data Points.

Fig 4.9 Finally Detected ECG peaks in the original ECG Wave.

Chapter 5

Arrhythmia Prediction using Machine Learning

5.1 Machine Learning And Its Importance

After calculation of the heart pulse , we use outputs R-R intervals and amplitude of R peaks to determine the condition of the patient with high accuracy .For this we need a large database to train the computer efficiently so that it accurately detects the state of the patient.

So for doing this , we are here using the SVM(Support Vector Machine) as a tool.

5.2 Support Vector Machine(SVM)

In machine learning, support-vector machines (SVMs, also support-vector networks) are supervised learning models with associated learning algorithms that analyze data used for classification and regression analysis. Given a set of training examples, each marked as belonging to one or the other of two categories, an SVM training algorithm builds a model that assigns new examples to one category or the other, making it a non-probabilistic binary linear classifier (although methods such as Platt scaling exist to use SVM in a probabilistic classification setting). An SVM model is a representation of the examples as points in space, mapped so that the examples of the separate categories are divided by a clear gap that is as wide as possible. New examples are then mapped into that same space and predicted to belong to a category based on which side of the gap they fall.

In addition to performing linear classification, SVMs can efficiently perform a non-linear classification using what is called the kernel trick, implicitly mapping their inputs into high-dimensional feature spaces.

When data is unlabelled, supervised learning is not possible, and an unsupervised learning approach is required, which attempts to find natural clustering of the data to groups, and then map new data to these formed groups. The support-vector clustering algorithm, created by Hava Siegelmann and Vladimir Vapnik, applies the statistics of support vectors, developed in the

support vector machines algorithm, to categorize unlabeled data, and is one of the most widely used clustering algorithms in industrial application

5.3 Working Of SVM

More formally, a support-vector machine constructs a hyperplane or set of hyperplanes in a high- or infinite-dimensional space, which can be used for classification, regression, or other tasks like outliers detection. Intuitively, a good separation is achieved by the hyperplane that has the largest distance to the nearest training-data point of any class (so-called functional margin), since in general the larger the margin, the lower the generalization error of the classifier

Whereas the original problem may be stated in a finite-dimensional space, it often happens that the sets to discriminate are not linearly separable in that space. For this reason, it was proposed¹ that the original finite-dimensional space be mapped into a much higher-dimensional space, presumably making the separation easier in that space. To keep the computational load reasonable, the mappings used by SVM schemes are designed to ensure that dot products of pairs of input data vectors may be computed easily in terms of the variables in the original space, by defining them in terms of a kernel function $k(x, y)$ selected to suit the problem. The hyperplanes in the higher-dimensional space are defined as the set of points whose dot product with a vector in that space is constant, where such a set of vector is an orthogonal (and thus minimal) set of vectors that defines a hyperplane. The vectors defining the hyperplanes can be chosen to be linear combinations with parameters α of images of feature vectors x that occur in the database. With this choice of a hyperplane, the points x in the feature space that are mapped into the hyperplane are defined by the relation $\sum_i \alpha_i k(x_i, x) = \text{constant}$. Note that if $k(x, y)$ becomes small as y grows further away from x , each term in the sum measures the degree of closeness of the test point x to the corresponding data base point x_i . In this way, the sum of kernels above can be used to measure the relative nearness of each test point to the data points originating in one or the other of the sets to be discriminated. Note the fact that the set of points x mapped into any hyperplane can be quite convoluted as a result, allowing much more complex discrimination between sets that are not convex at all in the original space

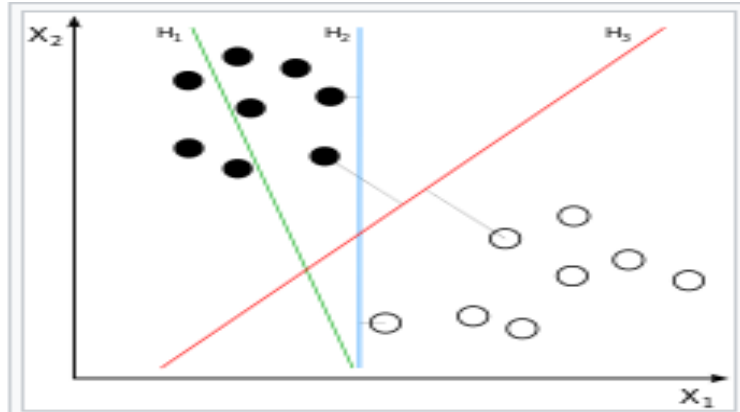


Fig 5.1 Classes separation using SVM

SVM classifier is used for our purpose to classify the training data from output. It is supervised learning method which analyses data with classification and regression analysis. As it can be inferred from above figures SVM finds hyper plane which classifies different kinds of data. We have chosen distance parameter to take into account the maximum length of data that can be considered in one class.

We have used SVM here over other machines since the data given is an imbalance data so for these kind datas the SVM works more accurately and precisely than others. Moreover it has less computational complexity and higher efficiency.

Here the database which is used to train the SVM is taken from two sources i.e., from MIT BHU database and data of the patients taken directly from hospitals. Over 3000 samples are taken with different heartbeats to train the SVM.

5.4 Results

- **SVC with Linear Kernel**

Description

SVM Kernel divides the given imbalanced data points into three different regions mainly:

Normal Heart Region data points are plotted in the blue region.

Ventricular Tachycardia data points are plotted in the red region.

Bradycardia data points are plotted in the brown region.

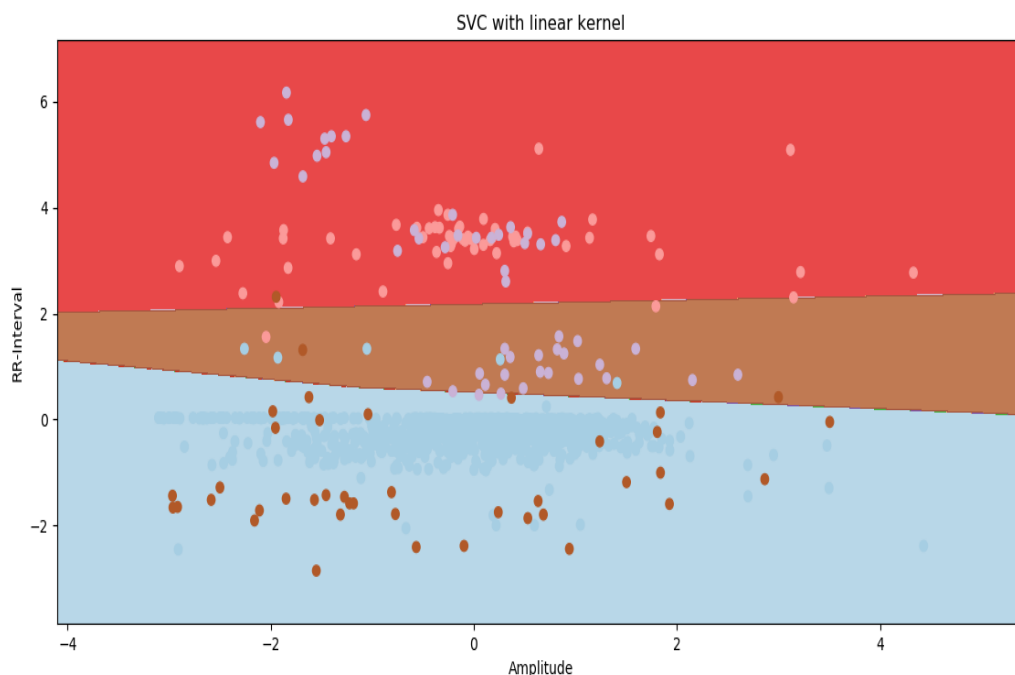


Fig 5.2 Formation of hyper planes by SVM

```
chandramouli@chandramouli-HP-Notebook:~/Documents/EEE/Project/ECG_DEMO$ python ecg.py
The input values of patient heart rate
Amplitude 1.1
RR interval 0.673
The patient has a Normal Sinus Heart Rate
```

Fig 5.3 Predicted Arrhythmia Condition for Given Patient Features using SVM.

Chapter 6

Hardware Implementation and Realisation of above Techniques

6.1 Hardware Requirements

- 3 ECG disposable lead electrodes.
- Probes
- CRO and USB to read the analog data.
- Capacitors as mentioned in the Circuit Diagram
- Resistors as mentioned in the Circuit Diagram
- 3 - Op-amps(IC 741) or (INA126 and TL071)
- Power Supply (15V, -15V).

6.2 Measurement Of Signals

- We have considered CRO for measuring the voltage values as it has high precision and accuracy with less error.
- We collected data from the CRO using USB .
- The raw data is converted from .dat file into .mat file and is further fed as input for Software Signal Processing.

ECG Signal is measured using disposable silver-lead ECG electrodes .

Signals from the arms and legs can be used to calculate the remaining Chest Voltage Signals from the formula given below

- Lead II = left leg - right arm
- Lead III = left leg - left arm (III = II - I)
- $avR = -\frac{1}{2}(I + II)$ (Chest Signal Voltages can be calculated from the above signals directly)
- $avL = I - \frac{1}{2}(II)$ (Chest Signal Voltages be calculated from the above signals directly)

- $avF = II - \frac{1}{2}(I)$ (Chest Signals Voltages be calculated from the above signals directly)
- Lead I = left arm - right arm



Fig 6.1 Measurement of ECG Signal using Disposable Lead Electrodes



Fig 6.2 ECG Signal Output in CRO

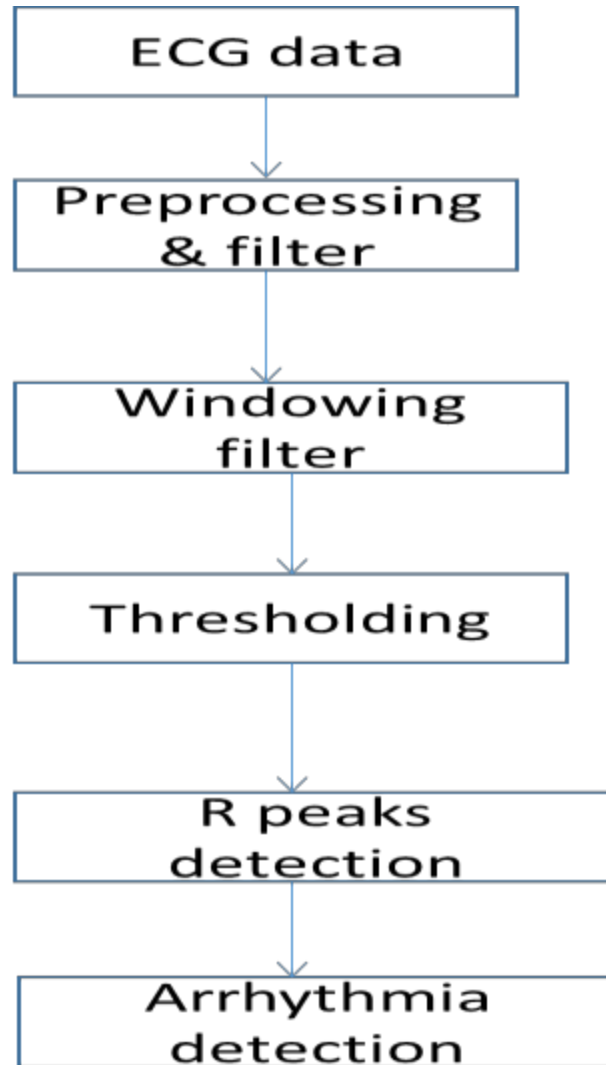


Fig 6.3 Block Diagram Of ECG Waveform R Peak Detection.

6.3 Amplifier (Two Stages)

6.3.1 Instrumentation Amplifier (First Stage)

- They are designed for good accuracy and for low-power application.
- Two op - amp topology reduces power consumption.
- A single external resistor can set the gain from 5 to 10000.
- It measures small differential voltage and high CMRR ratio.

- $G = 5 + 80k/R_g$.
- We have open circuited R_g which gives a Gain of 5.
- The output of the Instrumentation Amplifier is given to High Pass Filter which removes DC generated by the electrodes having cut off of 1 - 0.1 Hz.
- Blocking capacitors are inserted to prevent the amplifier oscillation.

6.3.2 Non Inverting Amplifier (Second Stage)

- Output of Instrumentation Amplifier is fed into the Non Inverting Amplifier.
- We set the Gain of an op - amp as $G = 1 + R_1/R_2$.
- We consider low resistor value for less noise.
- Feedback resistor is 100k for low power consumption.
- The cut off frequency is $f = 1/2\pi RC = 0.2\text{Hz}$. Otherwise the amplifier will amplify DC to saturation.

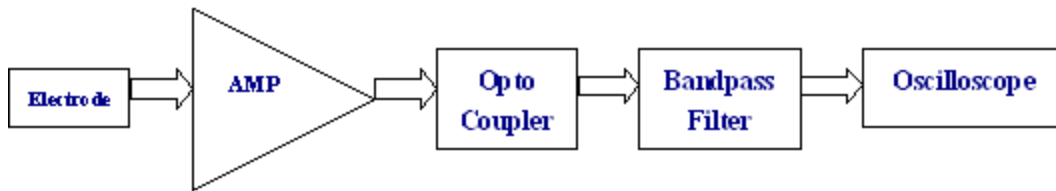


Fig 6.4 Block Diagram Of ECG Analog System

6.4 DWT vs FFT

- DWT Technique analyses the information in Three Dimensions (Frequency, Amplitude and Time) whereas FFT analyses the information in only Two Dimensions (Frequency and Time). So FFT generally uses lower number of computations compared to DWT.
- Denoising techniques can be applied to DWT techniques as both Amplitude and Frequency are being projected along Time axis which makes the removal of noises easier and to analyse the output data. FFT technique removes the frequency of signals which are not in the bandpass region. FFT technique doesn't bother about QST part of the wave and

focuses more on the R peaks whereas DWT cleans the entire signal so giving us more visually clean signal which can be used for analysis.

6.5 Advantages of Detecting ECG Peaks using these methods

- As hardware products evolve, the threshold values can be dynamically changed for software instead of having to modify heavy hardware equipments.
- Signal Processing in analog limits flexibility.
- Bandwidth, Gain and DC baseline are to be optimised in hardware.
- Digital filter implementation gives the designer flexibility to use adaptive dc removal filters for overall faster response and better rejection of baseline wandering.

6.6 Machine Learning (SVM Classifier) to Predict The Condition

$$\text{Heart Rate} = 60 * \text{Sampling rate} / (\text{R-R interval})$$

After calculating the heart pulse from the formula above, we use the outputs RR interval and Amplitude of R peaks to determine the condition of the patient using Machine Learning with high accuracy. With large given datasets and large conditions, it will be easier and accurate to predict the state of the patient.

Chapter 7

Conclusions

The heartbeat rate was detected using ECG signal processing techniques and Arrhythmia condition was detected using machine learning classification techniques(SVM). This method is a cost effective method as its cost is very less when compared to the ECG machine used in the hospitals. The main advantage of this method is it can be carried along with the person to all the places so that the heart condition of the patient can remotely analysed and if it is send to any doctor it quickly aid the people in abnormal condition. In this work, lightweight approach has been adopted to process the ECG signals from sensors in order to perform diagnosis based on a heart disease knowledge-base expert system. Our preliminary results demonstrated that the proposed model can remove noises from raw ECG signals, extract towards an IoT-based Expert System for Heart Disease Diagnosis. Key features were performed in support of the patients for pre-treatment and physicians for doing treatment. A proof-of-concept prototype of the proposed model towards building an IoT expert system has been implemented. However, there are several challenges to be addressed. These include the error detection and error correction of the collected data from sensors, online update of the knowledge-base to provide more precise diagnosis. To validate the proposed system with other independent validation mechanisms and datasets to ensure that the outcome of the present model is precise. Future instruments will focus more towards the user's emotional state and can be used to regulate information not only to collect them.

References

- [1] Alexakis.C. , Nyongesal.H.O. , Saatchi.R. , and Harris N.D., Dav.
- [2] A.V. Oppenheim, RW.Schafer and J.R. Buck. 2014. Discrete-time signal processing, 5th edition. Prentice hall.
- [3] El Mimouni, M. Karim. 2015. Novel Simple Decision Stage of Pan and Tompkins QRS Detector and its FPGA-Based Implementation. ISBN 978-1-4673-2679-7, pp. 331-336.
- [4] https://www.physionet.org/physiobank/database/ptbdb/patient001/S0010_re.
- [5] Izzah T.A., Alhady S.A., Ngah U.K. and Ibrahim W.P. 2013. A journal of real peak recognition of electrocardiogram (ecg) signals using neural network. American Journal of Networks and Communications. pp. 9-16.
- [6] <https://in.mathworks.com/help>.
- [7] N. Debbabi, S.El Asmi, H. Arfa. 2014. Real-time Correction of ECG baseline wander Application to the Pan and Tompkins QRS detection algorithm. IEEE.
- [8] Patel P.G., Warriar J.S. and Bagal U.R. 2012. ECG analysis and detection of arrhythmia using matlab. International Journal of Innovative Research and Development. 18(3): 59-68.
- [9] Sarkar. 2010. Elements of digital signal processing, Khanna publishers, Delhi, India.
- [10] Willis.J. Topkins 2012.Biomedical Processing, Prentice hall.
- [11] ECG Noise Sources and Various Noise Removal Techniques: A Survey. Mr. Hrishikesh Limaye1, Mrs. V.V. Deshmukh.
- [12] A Novel Approach For R-Peak Detection In The Electrocardiogram (ECG) Signal. B. Khaleelu Rehman, Adesh Kumar and Paawan Sharma.